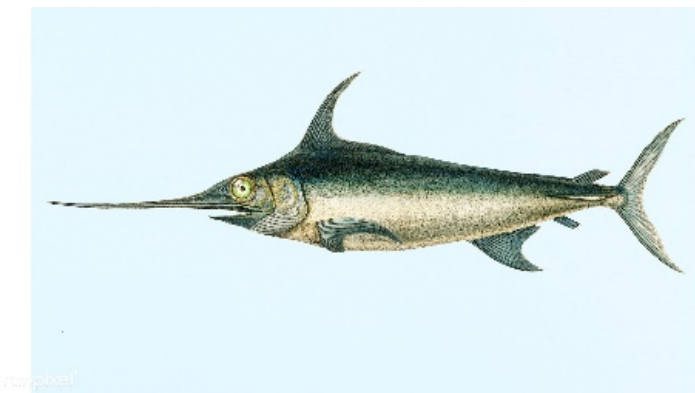


**Standardization of Western and Central North Pacific Swordfish
(*Xiphias gladius*) Catch Per Unit Effort in the Hawai'i Longline
Fishery from 1995–2021**

Erin Bohaboy and Michelle Sculley

National Marine Fisheries Service
1845 Wasp Boulevard
Honolulu, HI 96818

Email: michelle.sculley@noaa.gov



Abstract

The Western and Central North Pacific swordfish (*Xiphias gladius*) catch per unit effort for the Hawai'i-based longline fishery was standardized from the logbook dataset. The fishery was divided into the tuna-targeting deep-set sector and the swordfish-targeting shallow-set sector. Additionally, the shallow-set sector was standardized in two time periods: an early period (1995–2000) and a late period (2005–2021) because the shallow-set fishery was closed from 2001 to 2004, and regulations caused substantial changes in the fleet operations thereafter. Delta binomial-lognormal general additive models with random effects of fishing permit number as a proxy for vessel skill were evaluated for each sector and time-series. Spatial, temporal, environmental, and operational covariates were investigated for inclusion in the models following a forward stepwise approach based on Akaike Information Criteria and deviance explained selection criteria. The selected models explained between 34 and 49% of the deviance in the shallow-set sector and 31% of the deviance in the positive catches for the deep-set sector, but only 9% of the probability of presence/absence in the deep-set sector. Latitude and time of year were retained in all selected models, while time of day, moon phase, longitude, gear configuration (hooks per float), sea surface temperature, and bait type were also included in some models. The shallow-set standardized annual CPUE index displayed a general increasing trend from 1995–2000 and a decreasing trend from 2005–2021, with marked peaks in abundance in 2006 and 2016. Deep-set standardized annual CPUE estimates were an order of magnitude smaller than the shallow-set fishery and peaked in 1995, 2004, and 2015. Standardized CPUE indices for both fishery sectors have decreased over the last several years of the time-series, from 2016–2021 in the shallow-set sector and 2015–2020 in the deep-set sector.

Introduction

Broadbill swordfish (*Xiphias gladius*) inhabit the Pacific Ocean between 50° N and 50° S. They are a commercially important highly migratory species caught primarily by the Japanese, Taiwanese, and U.S. longline fisheries (Bigelow *et al.* 1999). The swordfish stock in the North Pacific Ocean has been assessed as a single stock scenario and under a two stock scenario, with one stock in the western central Pacific Ocean (WCNPO) and one stock in the eastern Pacific Ocean (EPO). These stocks were assessed in 2009 and again in 2014 by the Billfish Working Group (BILLWG) of the International Scientific Committee for Tuna and Tuna-like Species in the North Pacific Ocean (ISC) (ISC BILLWG 2009; ISC BILLWG 2014). The 2018 assessment of North Pacific swordfish only considered the WCNPO stock (ISC BILLWG 2019), and subsequent discussions with the Pacific Community and the Inter-American Tropical Tuna Commission (IATTC) redefined the EPO stock as a primarily southern stock. The southwest Pacific stock (SWPO) and the EPO stocks were assessed in 2021 and 2022, respectively (Ducharme-Barth *et al.* 2021; Minte-Vera *et al.* 2022).

The BILLWG of the ISC has proposed to attempt a benchmark assessment of North Pacific swordfish in 2023. In preparation for the assessment, this working paper describes the standardization of swordfish catch per unit effort (CPUE) from the Hawai'i-based longline fleet where swordfish are caught as targeted-species in the shallow-set sector (float lines less than 20 m in length to allow fishing closer to the surface, with 14 or fewer hooks per float) and as bycatch in the tuna-targeting deep-set sector (float lines 20 m in length or greater to allow fishing at greater depths, with at least 15 hooks per float).

Historically, the Hawaiian longline fishery targeted tuna; however, in the early 1990s the number of vessels targeting swordfish began increasing and the Hawai'i-based fleet

accounted for 40% of the total U.S. swordfish catch in 2012. Observers were first placed onboard longline vessels in 1994. Interactions with protected sea turtles caused the closure of the shallow-set swordfish fishery from February 2001 to March 2004 (Gilman *et al.* 2007). During this time many vessels targeting swordfish began targeting tuna. A second closure occurred March–December 2006 when the Hawai’i-based shallow-set longline fishery for swordfish reached the annual limit for interactions with loggerhead sea turtles, and additional closures of the fishery have occurred in recent years (NMFS 2022). Several changes to the reporting regulations have occurred since the onset of required reporting in 1994 (Pacific Islands Region Office 2017). Observer coverage varied significantly prior to 2000, with observer coverage between 3.3 and 10.4% for the entire fishery (NMFS 2022). Starting in 2001, the observer program had a target of 20% observer coverage on deep-set longline vessels and mandatory 100% observer coverage on shallow-set longline vessels. The Hawai’i-based longline fleet has been described previously by Ito and Childers (2018) and also in a working paper submitted to the same BILLWG session (Ito 2023) and there have not been additional substantial changes since 2018.

Methods

Data Sources

The U.S. Federal logbook program to monitor the Hawai’i-based longline fishing fleet began in November 1990 to manage U.S. domestic fisheries for tuna, swordfish, and other economically important pelagic species. Logbooks are filed by all operators of fishing vessels conducting longline fishing operations on the High Seas and within the U.S. Exclusive Economic Zone in American Samoa, Guam, Hawai’i, the Northern Mariana Islands, and U.S. possessions in the western Pacific and offloading in U.S. ports. Logbooks provide set-by-set information on catch, as well as environmental and operational aspects of fishing operations. The Hawai’i-based longline fishery can be divided into two sectors: the tuna-targeting deep-set sector which comprises the majority of the fishing fleet, and the swordfish-targeting shallow-set sector. Data were extracted from the Oracle database on 2 September 2022. After filtering for incomplete and erroneous entries, there were 424,715 longline sets available for inclusion in these analyses from 10 June 1995 to 31 December 2021.

Target species are not consistently reported for each longline set in logbook records. Target species (hence fishery sector: deep- vs. shallow-set) were instead inferred by the number of hooks per float (HPF). Prior to the close of the shallow-set sector in 2001, we defined shallow-sets as sets having 10 or fewer HPF. After the reopening of the shallow-set fishery in 2005, Shallow-sets were legally defined as having 14 or fewer HPF in 2004 (69 FR 17329), and we use that definition for the 2005–2021 shallow-set time-series. Consistent with the 2004 definitions, we defined deep-sets over the time-series (1995–2021) as sets with 15 or more HPF. Prior to 2001, sets with 11–14 HPF ($N = 573$ sets, or approximately 0.1% of all records) could not be confidently assigned to either sector and have been removed from the dataset for these analyses.

The environmental variables investigated in the CPUE standardization were obtained from publically available data. Sea surface temperature (SST) from January 1994 to present were based on monthly 0.5° resolution composites from the NOAA GOES-E/W satellite downloaded from Pacific Islands Fisheries Science Center (PIFSC) OceanWatch (2022). The Southern Oscillation Index (SOI) and the Pacific Decadal Oscillation Index (PDO) were monthly region-wide indices (NOAA NCDC 2022). Mixed layer depth (MLD) were based on $0.33^\circ \times 1^\circ$ monthly means of GODAS data provided by the NOAA/OAR/ESRL PSD,

Boulder, Colorado, USA¹. Latitude and longitude were the calculated Euclidian mid-point between the locations recorded for the beginning of longline set and end of longline haulback. Lunar phase was assigned for each set using the R package ‘lunar’ (Lazaridis 2015) providing values between 0 and 1 with 0 and 1 as the beginning and end of the moon cycle (new moon), 0.25 as the first quarter, 0.5 as the full moon, and 0.75 as the last quarter. Potential seasonal effects on catch rates were accounted for with a day of year value ranging from 1 to 365 (or 366 during leap years). Time of day for each set was the time when the longline deployment began and was measured by hour from 0 to 23. HPF was treated as a categorical variable with integer values for shallow-sets and increments for deep-sets (15–20, 21–25, 26–30, …, 55–88). The logbook data included over 40 recorded bait types, which were reduced to 8 categories: 1. mackerel, 2. various mixed species (including various combinations of squid, mackerel, saba, sanma, sardine, akule, opelu, and herring), 3. all other species or unknown baits, 4. saba, 5. sanma, 6. sanma/sardine mix, 7. sardine, and 8. squid. Finally, a measure of set effort in total number of hooks was investigated for some standardization some models.

CPUE Standardization

Catch per unit effort (CPUE) was measured as the count of swordfish caught per 1000 hooks set. Each dataset (shallow-set 1995–2000, shallow-set 2005–2021, and deep-set 1995–2021) was modeled separately as the combination of presence/absence (binomial distributed) and positive catch (lognormal distributed) processes. A presence/absence model was not considered for the shallow-set 2005–2021 standardization because sets catching no swordfish were rare (1.1% of all sets). Instead, the CPUE index was standardized based on the lognormal model of positive catches only. This carries the assumption that the probability of catching swordfish in this sector was essentially constant at 1 throughout the time-series. Each process was modeled with a general additive mixed-effects model (GAMM) in R package ‘gamm4’ (Wood *et al.* 2020) where vessel permit number (a unique identifier that can be used as a proxy for fishing vessel) was included *a priori* in all models as a random effect to account for possible changes in vessel fishing capability (skill) over time.

Eleven covariates were investigated for inclusion in the GAMMs. Bait type and HPF were considered as categorical variables; SST, SOI, PDO, and MLD were considered as linear terms, latitude and longitude were considered as thin plate regression spline smoothed terms, and moon phase, time of year, and time of day were considered as cyclic cubic regression splines. Cyclic cubic regression splines were penalized to ensure model effects for minimum and maximum values of each covariate matched, *e.g.* 0 and 1 for moon phase, 0 and 366 for time of year, and 0 and 24 for time of day. The dimension of the basis (*e.g.*, maximum number of knots) for all smooth terms was 6–8. Models were selected using a forward stepwise approach. All perspective covariates were evaluated at each step (total effort in number of hooks per set was considered only for the binomial presence/absence models). Models containing each candidate covariate were compared to the previous step using a chi-squared likelihood ratio test (Ott and Longnecker 2001). The model with the lowest Akaike information criterion (AIC) value and a significant likelihood ratio test statistic at alpha = 0.05 was retained at each step. Addition of covariates to each model continued only if the percent deviance explained relative to the intercept only (null) model was at least 0.25% greater than the percent deviance explained by the next simplest model. Residual distributions for each selected presence/absence and positive process model, as well as marginal effects (computed using R package ‘ggeffects’; Ludecke *et al.* 2022) for each

¹ <http://www.esrl.noaa.gov/psd/>

covariate were examined to ensure model appropriateness. The influence of each covariate on the predicted values within each GAMM were plotted and examined following Bentley *et al.* (2012) to illustrate trends in covariate effects on CPUE over time.

The annual probability of presence/absence (binomial process) and expected CPUE given positive catch (lognormal process), together with variance estimates, were calculated for all combinations of year × month × categorical variable (either HPF or Bait) included in the model of each time-series (Walters 2003). Median values for linear and smooth covariates were also used in the predictions. Marginal mean values and variances were calculated by year and, for the shallow-set 1995–2000 and deep-set 1995–2021 time-series, combined following the approach of Goodman (1960) as described in Campbell (2015) to produce the final standardized CPUE indices.

Results

Descriptive Catch Statistics

Swordfish-targeting shallow-set longline fishing activity from 1995–2021 was centered 2–3° latitude north of the western Main Hawaiian Islands (MHI) and extended farther north along the North Pacific Subtropical Convergence Zone (Figure 1). Prior to the shallow-set fishery closure in 2000, most shallow-set effort was relatively close to the north and south of the MHI, however, since 2005, the spatial extent of shallow-set effort has been reduced and generally shifted north and east which coincided with the creation of the Papahānaumokuākea Marine National Monument in 2006 and its subsequent expansion in 2016 around the Northwest Hawaiian Islands (Figure 2 and Figure 3). Nominal CPUE aggregated over the time-series is highest along the North Pacific Subtropical Convergence Zone above the Northwest Hawaiian Islands (Figure 4). Areas of the highest nominal CPUE have been fairly consistent over time, but have shifted farther east in recent years (Figure 5 and Figure 6).

Prior to the shallow-set fishery closure in 2001, shallow-set fishing occurred throughout the year (Figure 7A). During the latter time-series, effort tended to be concentrated within the first months of the year. This seasonal concentration of effort is particularly noticeable during years when the fishery was closed mid-year due to sea turtle interactions (e.g., 2006, 2018, 2019). During the early time-series (1995–2000), shallow-set longlines were set throughout the day, but mostly between 1600 and 1800 (Figure 7B). The setting of shallow-set longlines from 2005–2021 was later, consistent with regulations enacted in 2004 prohibiting shallow-setting within 1 hour after sunset, and effort was concentrated from 1800–2000 during most years. Shallow-set effort has become increasingly focused around the full moon in recent years (Figure 7C). The spatial shift of the fishery to the north and east over the years, as well as increased variability of the set location in recent years are apparent from the relative frequency of sets per year by latitude (Figure 7D) and longitude (Figure 8A). Finally, there was a pronounced shift in fishermen behavior in 2010–2011 (Figure 8B). In years earlier, shallow-sets most commonly had 4 HPF, but since 2012 most sets used 5 HPF.

Tuna-targeting deep-set longline fishing activity was concentrated close to MHI and has expanded to the north and east over the time-series (Figure 9–Figure 11). Nominal CPUE was most often < 0.2 through the range of the deep-set fishery (Figure 12), with the exception of relatively high CPUE values (range 1–15.3), primarily in the North Pacific Subtropical Convergence Zone during 1996, 2001–2002, and 2011–2012 (Figure 13 and Figure 14). Deep-set fishing occurred throughout the year with set times between 0600 and noon, shifting later over time (Figure 15A–B). The number of deep-sets by latitude and SST have been highly

variable over time, with no apparent trend (Figure 15C–D). Consistent with regulations, squid has not been used as a bait in the deep-set sector since 2002, with sanma increasingly the preferred bait type (Figure 16A). Deep-set HPF decreased from a mode of 31–35 before 2004 to 21–25 after 2007 (Figure 16B).

CPUE Standardization

Time of day, time of year, latitude, and HPF were selected for both the presence/absence and positive catch GAMMs for the 1995–2000 shallow-set fishery (Table 1). In addition, the positive process model included moon phase and longitude. Both models explained approximately 48–49% of deviance compared to the null (intercept only) model. The 2005–2021 shallow-set fishery was modeled using only the positive process GAMM (34.4% of deviance explained) and included moon phase, time of year, SST, longitude, and latitude. Time of year, SST, and latitude were selected for both the presence/absence and positive catch GAMMs for the deep-set fishery. In addition, the positive process model included time of day, bait, and HPF. The presence/absence GAMM for the deep-set fishery explained only 8.8% of deviance compared to the null (intercept only) model, while the positive process GAMM explained 30.9% of deviance.

Annual standardized CPUE for the 1995–2000 shallow-set fishery followed an increasing trend over the time-series (Figure 17). CPUE for the 2005–2021 shallow-set fishery peaked in 2006 and 2016, and has been trending down to minimum 7.20 per 1,000 hooks in 2021 (Table 2). Annual standardized deep-set CPUE has been less than 0.2 per 1,000 hooks in all except 2 years, peaking in 1995, 2004, and 2015 (Figure 18). Similar to the shallow-set standardized CPUE, the deep-set standardized CPUE exhibits an overall decreasing trend in recent years, reaching time-series minimum values of 0.10 and 0.11 per 1,000 hooks in 2020 and 2021, respectively (Table 2). Diagnostic plots of each of the final selected GAMMs indicate residuals are roughly normally distributed and show no distinct trends (Figure 19–Figure 23).

Time of day, time of year, and latitude had similar effects and influence within both the presence/absence and positive process GAMMs for the 1995–2000 shallow-set fishery (Figure 24–Figure 27). Marginal effects were most positive (hence the probability of catching swordfish and the CPUE given swordfish were caught was highest) around 1800 hours, spring/early summer, and 30–40° N latitude. Further, the effects of time of day and time of year showed positive influence trend over time, indicating including these variables in the standardization models accounted for a positive trend that would have been influential in the nominal CPUE time-series. For the 2005–2021 shallow-set fishery, which was modeled using only a positive process GAMM, the effects of time of year and latitude were similar to the earlier time-series, *e.g.*, effect was highest in March and approximately 35–40° N latitude (Figure 28). Moon phase had the greatest positive effects on CPUE several days before the full moon and the range of marginal effects for permit was greater than for the 1995–2000 time-series. The effects of longitude suggest a gradient from greatest in the west to least in the east. Trends in influence over time were positive for the effects of moon phase and latitude, but were negative for longitude (Figure 29).

Relative to the shallow-set fisheries, permit effect was more pronounced for both the presence/absence and positive process GAMMs for the 1995–2021 deep-set fishery (Figure 30 and Figure 32). Interestingly, the trends in influence of permit over time were opposite for the two processes, being positive for the presence/absence process and negative for the positive process (Figure 31 and Figure 33). The marginal effect of year showed high variability and no trend for the presence/absence process but was negative for the positive process.

Trends in CPUE were similar to trends observed in the previous 2018 CPUE standardization (Figure 34 and Figure 35; Sculley *et al.* 2018). Both the previous and current indices displayed an increase for the shallow-set fishery from 2013–2016 and the deep-set fishery from 2011–2015. Beyond the 2016 terminal year of the 2018 standardization, CPUE for both shallow-set and deep-set fisheries has generally declined.

Discussion

Latitude and time of year were consistently selected in the GAMMs for the presence/absence and positive processes of both the shallow- and deep-set fishery sectors. The importance of spatial covariates in the models was expected given catch rates of swordfish are known to be highest near oceanographic features such as frontal currents, eddies, and upwelling and convergence zones, including the North Pacific Subtropical Convergence Zone north of the Hawaiian Islands (Yanez *et al.* 2009; Sculley *et al.* 2019; Duran Gomez *et al.* 2020). Previous analyses of Hawai'i longline logbook data also demonstrated the importance of spatial covariates to swordfish catch rates (Bigelow *et al.* 1999; Sculley *et al.* 2018). In this analysis, latitude and longitude were accounted for in the models as additive, rather than linear, terms, and were selected earlier in the most parsimonious models compared to the previous CPUE standardization analysis (Sculley *et al.* 2018). This suggests that additive effects allow for more realistic modeling of spatial covariates, allowing for maxima or minima at intermediate latitude and longitude values instead of a single maximum and minimum at the extent of the data indicative of a unidirectional relationship. Longitude was not selected in any of the models in the 2018 CPUE standardization, despite relying on identical model selection criteria as the current analysis. An earlier analysis of swordfish catch data by Bigelow *et al.* (1999) using only a few years of longline logbook data retained longitude in the CPUE standardization models, but there was no clear east-west trend. In addition to the more flexible treatment of longitude using additive modeling, the years 2017–2021 were informative regarding the east-west distribution of fishing effort in the shallow-set fishery, which has moved farther to the east where catch rates are expectedly lower in response to the periodic regulatory closure of the bigeye tuna fishery (Russ Ito, pers. comm.), corresponding to large negative influence of longitude for those years (Figure 29). Although we tested for interactions between latitude and longitude in the GAMMs that retained both terms, interactions were not included in the final models in the interest of reducing the number of parameters. Future improvements to the CPUE standardization of Hawai'i longline logbook data include modeling spatial effects using 1° latitude × longitude grid cells and investigating year × space interactions.

Time of year was considered at a finer resolution (day of year) and more flexibly as an additive term, rather than the 4-level categorical season in the 2018 CPUE standardization. Time of year was selected as the first or second covariate in all GAMMs. The effect of time of year on shallow-set CPUE is particularly apparent in 2006, 2018, and 2019 when the shallow-set sector was closed early (in March, May, and March, respectively). During these years, all shallow-set effort occurred during the beginning of the year when marginal effects of season (time of year) were most positive, hence influence of time of year was strongest during those years (Figure 7Figure 28Figure 29). For the deep-set fishery, the probability of encountering swordfish, as well as CPUE of swordfish given they were caught, was highest during April through June (Figure 30 Figure 32). As expected, influence of time of year is greatest for years when more deep-set fishing effort coincides with these peak months (Figure 31Figure 33). The converse is also apparent: logbook data became available in June 1995, as a result, all observed fishing effort for 1995 was during times when CPUE of swordfish from both the shallow-set and deep-set fisheries was expected to be low. Intuitively, influence plots

show strong negative influence of time of year on CPUE in 1995 within both the presence/absence and binomial GAMMs for the shallow- and deep-set sectors (Figure 25Figure 27Figure 31Figure 33).

General trends in the standardized CPUE index for both the shallow-set and deep-set sectors indicate a peak approximately every 10 years, while the shallow-set peaks lagged 1 year behind the deep-set peaks. The signal in the deep-set sector is very small as the CPUE ranges from 0.1 to 0.19 between 1996 and 2021. This sector catches primarily young-of-the-year fish with a mean length of 80 cm EFL (Brodziak and Sculley 2023). Neither the PDO, which cycles approximately every 10 years, or the SOI, which cycles more frequently, were retained in any of the models, noting that neither index was offset by time (e.g., PDO in a given year was investigated for model effects on catch of the same year). This suggests that although largescale climatic indices may potentially be driving underlying swordfish abundance and recruitment (which cycles every 7–8 years; ISC BILLWG 2019), largescale climate variability is apparently not driving catchability of swordfish within the Hawai‘i longline fisheries. Future investigations of environmental influences on catchability of swordfish could rely on wind data as a more reliable indicator of fishing conditions, as was done by Bigelow *et al.* (1999).

The influence of SST and MLD on the catch rates and local density of swordfish is well documented (Bigelow *et al.* 1999; Abascal *et al.* 2015), therefore, it is surprising MLD was not retained in any of the GAMMs and SST had only very subtle effects with large variance. This is likely the result of confounding caused by correlation between SST and MLD with spatial and seasonal variables. The direction and magnitude of the correlation between MLD and latitude or longitude varied depending on the fishery sector and time period considered. Considering shallow-sets only, MLD was positively correlated with latitude (Pearson correlation $\rho = 0.18$) and longitude ($\rho = 0.44$) but for deep-sets, MLD was negatively correlated with latitude ($\rho = -0.47$) and longitude ($\rho = -0.26$). SST was not strongly correlated with latitude or longitude within the data (strongest $\rho = -0.18$ between SST and latitude for the shallow-set data), however, SST was correlated with time of year ($\rho = 0.47$). MLD was negatively correlated with time of year ($\rho = -0.48$). The seeming unimportance of SST and MLD represents a primary difference between this and the 2018 analyses which included SST in 4 of 5 and MLD in 3 of 5 GLMs using the same model selection criteria. The flexible inclusion of time of year and space at much finer resolution in these analyses likely enabled seasonal and spatial variables to account for a greater amount of the deviance.

Moon phase was found to be an important covariate associated with CPUE for the shallow-set fisheries. In both time-series, the effect of moon phase is most strongly positive several days before (moon phase = 0.4 to 0.45) and, to a lesser extent, several days after (moon phase = 0.65) the full moon, and not during the full moon itself (moon phase = 0.5). This suggests either there is an optimum level of illumination at about 70–90% full that maximizes swordfish interaction with longline gear; or, as might be suggested by the asymmetry of the relationship, perhaps indirect ecological or behavioral mechanisms cued by moon phase are driving the increased catches of swordfish during these times. Regardless, the frequency plots reveal that shallow-set effort is concentrated around the full moon, and in some years peaks several days before or after the full moon (Figure 7). Moreover, effort has been increasingly concentrated between the first and last quarter moons over the time-series, and the influence of moon phase within the CPUE standardization GAMMs trended positively (Figure 29).

Vessel (permit) effect, as a proxy for fishermen skill or efficacy, was included as a random effect *a priori* in all GAMMs. For the shallow-set fishery, the range of the marginal effect within the GAMMs was small in the presence/absence process (Figure 24) and fairly large in

the positive processes (Figure 26 and Figure 28), suggesting whether or not swordfish are caught during a shallow-set is not heavily dependent on vessel, however, given swordfish are caught, the number caught is affected by the vessel. Vessel was a prominent covariate within both processes for the deep-set fishery (Figure 30Figure 32). There were a few vessels in particular that seemed much more likely to catch swordfish, or catch more swordfish, than other vessels, suggesting there are a few vessels that are better able to catch (or less able to avoid) swordfish on deep-sets. Industrialized fishing fleets become more skilled overtime, either by individual fishermen adopting new technologies and behaviors or attrition of less successful fishermen (Eigaard *et al.* 2014). Including vessel can account for the attrition of less skilled fishermen over time, and, as observed by Bentley *et al.* (2012), the influence of vessel within the standardization model may increase over time in targeted fisheries. Instead, we found influence of the permit effect within the shallow-set fishery was highest in the middle of the time-series (2013–2017; Figure 29). Influence of vessel in the deep-set fishery trended positively over time for the presence/absence process (*e.g.*, the composition of the fleet is tending towards vessels that catch swordfish on deep-sets; Figure 31) and decreased until 2004 then stabilized for the positive process (*e.g.*, the composition of the fleet is moved towards vessels that, when swordfish are caught, do not catch many swordfish on deep-sets since the regulatory changes of 2004; Figure 33).

Of the investigated operational covariates, HPF was the most commonly included. However, for all three selected models that included HPF (shallow-set 1995–2000 presence/absence, shallow-set 1995–2000 positive process, and deep-set positive process), HPF was the last covariate selected, accounting for an additional 0.34, 0.42, and 0.26 percent of deviance explained, respectively, which was very slightly above the threshold of 0.25 percent for inclusion of additional terms. For the shallow-set fishery, marginal effects of HPF suggest using 9 HPF had a negative effect on both the probability of a positive catch and CPUE, while using most other numbers of HPF had a positive effect (Figure 24Figure 26). For deep-sets, CPUE was somewhat higher when 45–49 or 50–54 HPF were used (Figure 32). Given that the confidence intervals of effects at each level of HPF generally overlap and the great majority of shallow-sets used 4, then 5 HPF (shifting around 2009–2011; Figure 8) and most deep-sets used 30–34 HPF (decreasing to 25–29 HPF later in the time-series; Figure 16), inferences drawn on HPF within the GAMMs are likely unreliable. Bait type was also a challenging covariate to account for or interpret in the selected GAMMs, appearing only in the deep-set positive process model where mackerel and squid (which are the favored baits for targeting swordfish; Fernandez-Carvalho, et. al., 2015) indicated higher CPUE compared to the other bait categories (Figure 32), which included over 40 bait types, frequently mixed within sets and not recorded specifically in the logbook data.

The standardized CPUE for both the shallow- and deep-set fisheries has trended down over the terminal 5–7 years of the time-series. This decrease in CPUE could not be explained by any of the spatial, temporal, environmental, or operational covariates investigated here. As noted, the recent downward trend could be the continuation of a regular 10-year cycle in CPUE, perhaps driven by the environment and cycles in recruitment (ISC BILLWG 2019). Whether this recent decrease in CPUE is indicative of a decrease of abundance of the overall WCNPO swordfish stock will be thoroughly investigated in the upcoming benchmark stock assessment. Given the close agreeance of this and the previous CPUE standardization through 2016, it is likely the recent trends are similarly reliable as the earlier part of the time-series.

In conclusion, we believe the standardized CPUE indices from the Hawai'i longline logbook data presented herein represent a methodological improvement over the previous analyses (Sculley *et al.* 2018). In particular, the flexibility of additive modeling, greater resolution of modeling time of day and time of year as continuous variables, and the consistent inclusion of

a random effect for fishermen skill more realistically reflect the relationship between the investigated covariates and logbook catch. Future improvements could be made to the analyses, including better accounting for spatial variation, and incorporating spatiotemporal interactions. Regardless, model diagnostics indicate the delta-lognormal modeling approach with the covariates selected are appropriate to quantify the underlying year effect on swordfish catch.

Literature Cited

- Bentley, N., Kendrick, T. H., Starr, P. J., and Breen, P. A. 2012. Influence plots and metrics: tools for better understanding fisheries catch-per-unit-effort standardizations. ICES Journal of Marine Science 69(1): 84–88. doi:10.1093/icesjms/fsr174.
- Bigelow, K. A., C. H. Boggs and He, X. I. 1999. Environmental effects on swordfish and blue shark catch rates in the US North Pacific longline fishery. Fisheries Oceanography 8(3): 178-198.
- Campbell, R.A. 2015. Constructing stock abundance indices from catch and effort data: some nuts and bolts. Fisheries Research 161:109–130. doi:10.1016/j.fishres.2014.07.004.
- Ducharme-Barth, N., C. Catillo-Jordan, J. Hampton, P. Williams, G. Pilling, and Hamer, P. 2021. Stock assessment of southwest Pacific swordfish. WCPFC-SC17-2021/SA-WP-04. 151 pp.
- Durán Gómez, G.S., Nagai, T., and Yokawa, K. 2020. Mesoscale warm-core eddies drive interannual modulations of swordfish catch in the Kuroshio Extension System. Frontiers in Marine Science 7:1–20. doi:10.3389/fmars.2020.00680.
- Eigaard, O.R., Marchal, P., Gislason, H., and Rijnsdorp, A.D. 2014. Technological development and fisheries management. Reviews in Fisheries Science and Aquaculture. 22(2):156–174. doi:10.1080/23308249.2014.899557.
- Joana Fernandez-Carvalho, J., Coelho, R., Santos, M.N., and Amorim, S. 2015. Effects of hook and bait in a tropical northeast Atlantic pelagic longline fishery: Part II—Target, bycatch and discard fishes. Fisheries Research 164:312-321. doi: 10.1016/j.fishres.2014.11.009.
- Gilman, E., D. Kobayashi, T. Swenarton, N. Brothers, P. Dalzell and Kinan-Kelly, I. 2007. Reducing sea turtle interactions in the Hawaii-based longline swordfish fishery. Biological Conservation 139(1–2): 19-28.
- Goodman, L.A. 1960. On the exact variance of products. Journal of the American Statistical Association. 55(292):708–713.
- ISC BILLWG. 2009. Report of the billfish working group workshop (Annex 7). International Scientific Committee for Tuna and Tuna-like Species in the North Pacific Ocean 19–26 May 2009. Busan, Korea.

- ISC BILLWG. 2014. North Pacific Swordfish (*Xiphias gladius*) Stock Assessment in 2014. International Scientific Committee for Tuna and Tuna-like Species in the North Pacific Ocean 16-22 July 2014. Taipei, Chinese-Taipei.
- ISC BILLWG. 2019. Stock Assessment for Swordfish (*Xiphias gladius*) in the Western and Central North Pacific Ocean through 2016. International Scientific Committee for Tuna and Tuna-like Species in the North Pacific Ocean 11–16 July 2018. Yeosu, Republic of Korea.
- Ito, R.Y. and Childers, J. 2018. US Swordfish Fisheries in the North Pacific Ocean. ISC/18/BILLWG-01/01.
- Ito, R.Y. 2022. US Swordfish Fisheries in the North Pacific Ocean.
- Lazaridis, E. 2015. R Package “lunar”: lunar phase & distance, seasons and other environmental factors. Available from <https://cran.r-project.org/web/packages/lunar/lunar.pdf>.
- Ludecke, D., Aust, F., Crawley, S., and Ben-Shachar, M.S. 2022. Package “ggeffects”: create tidy data frames of marginal effects for “ggplot” from model outputs. Available from <https://cran.r-project.org/web/packages/ggeffects/ggeffects.pdf>.
- Minte-Vera, C.V., M.N. Maunder, H. Xu, C.E. Lennert-Cody, J.L. Valero, and Aires-da-Silva, A. 2022. South EPO swordfish benchmark assessment: progress report. Inter-American Tropical Tuna Commission Scientific Advisory Committee Meeting. 16-20 May, 2022. La Jolla, California, USA. SAC-13-09. 3 pp.
- NMFS. 2022. Hawaii longline fishery logbook statistics -non-confidential summary tables. Available online at <http://www.pifsc.noaa.gov/fmb/reports.php>, accessed 1 October 2022. National Marine Fisheries Service, Pacific Islands Fisheries Science Center, Honolulu.
- NOAA NCDC 2022. Spatially and temporally large-scale anomalies that influence the variability of the atmospheric circulation. Online Database <https://www.ncdc.noaa.gov/teleconnections/> Accessed 05 September 2022.
- Ott, R.L., and Longnecker, M. 2001. An Introduction to Statistical Methods and Data Analysis. 5th edition. Duxbury Thomson Learning, Pacific Grove, California.
- Pacific Islands Fisheries Science Center (PIFSC) OceanWatch. (2022) Central Pacific Node. <http://pifsc-oceanwatch.irc.noaa.gov/> Accessed: 05 September 2022.
- Pacific Islands Region Office (PIRO). 2017. Hawaii Longline Observer Program Observer Field Manual. Version LM.17.02. National Oceanic and Atmospheric Administration, Pacific Islands Region, Honolulu, Hawai‘i.
- Sculley, M., A. Yau, and M. Kapur. (2018). Standardization of the Swordfish (*Xiphias gladius*) Catch per Unit Effort Data Caught by the Hawaii-based Longline Fishery from 1994–2017 Using Generalized Linear Models. ISC/18/BILLWG-01/02.

- Sculley, M. (2019). Standardization of the Striped Marlin (*Kajikia audax*) Catch per Unit Effort Data Caught by the Hawaii-based Longline Fishery from 1994–2017 Using Generalized Linear Models. ISC/19/BILLWG-01/06.
- Walters, C. 2003. Folly and fantasy in the analysis of spatial catch rate data. Canadian Journal of Fisheries and Aquatic Sciences. 60(12):1433–1436. doi:10.1139/f03-152.
- Winker, H., Kerwath, S.E., and Attwood, C.G. 2013. Comparison of two approaches to standardize catch-per-unit-effort for targeting behaviour in a multispecies hand-line fishery. Fisheries Research 139:118–131. doi:10.1016/j.fishres.2012.10.014.
- Wood, A.S., Scheipl, F., and Wood, M.S. 2020. Package ‘gamm4’: Generalized additive mixed models using ‘mgcv’ and ‘lme4’. Available from <https://cran.r-project.org/web/packages/gamm4/gamm4.pdf>.
- Yáñez, E., Silva, C., Barbieri, M.A., Órdenes, A., and Vega, R. 2009. Environmental conditions associated with swordfish size compositions and catches off the Chilean coast. Latin American Journal of Aquatic Research. 37(1):71–81. doi:10.3856/vol37-issue1-fulltext-6.

Tables

Table 1. Selected models used in the CPUE standardization. All models included year and random effects of permit. Additive (smooth) terms are noted by s(). Model covariates include hour (Hour), day of year (Yday), latitude (Lat), longitude (Lon), hooks per float (HPF), moon phase (Moon), sea surface temperature (SST), and bait type (Bait).

Form / Process	Model Covariates	% Deviance Explained	Comments
Shallow-set, 1995–2000 ($N = 24,233$; 14.7% zeros)			
GAMM presence / absence	s(Hour) + s(Yday) + s(Lat) + HPF	48.4	Lon and Moon were eliminated from consideration after Lat was selected due to convergence failure.
GAMM positive process	s(Lat) + s(Yday) + s(Moon) + s(Lon) + s(Hour) + HPF	48.9	
Shallow-set, 2005–2021 ($N = 18,723$; 1.1% zeros)			
GAMM positive process	s(Moon) + s(Yday) + SST + s(Lon) + s(Lat)	34.4	
Deep-set, 1995–2021 ($N = 380,915$; 84.2% zeros)			
GAMM presence / absence	s(Yday) + SST + s(Lat)	8.8	Model selection performed using a subset of data (5%)
GAMM positive process	s(Hour) + s(Yday) + Bait + s(Lat) + SST + HPF	30.9	

Table 2. Annual standardized CPUE (number per 1000 hooks) and CVs.

Year	Shallow-set		Deep-set	
	CPUE	CV	CPUE	CV
1995	6.36	0.09	0.30	0.12
1996	6.85	0.09	0.19	0.11
1997	7.80	0.1	0.12	0.12
1998	7.85	0.1	0.17	0.11
1999	7.69	0.08	0.15	0.11
2000	8.07	0.08	0.13	0.11
2001			0.14	0.11
2002			0.18	0.11
2003			0.16	0.11
2004			0.21	0.10
2005	15.25	0.09	0.15	0.11
2006	16.87	0.08	0.16	0.11
2007	14.16	0.09	0.15	0.11
2008	13.20	0.09	0.14	0.11
2009	10.69	0.09	0.15	0.11
2010	9.74	0.09	0.13	0.11
2011	10.69	0.09	0.11	0.11
2012	9.28	0.09	0.13	0.11
2013	9.31	0.09	0.13	0.11
2014	9.51	0.09	0.17	0.10
2015	10.61	0.09	0.18	0.10
2016	12.29	0.09	0.15	0.10
2017	12.19	0.09	0.16	0.10
2018	10.22	0.09	0.16	0.10
2019	8.86	0.09	0.13	0.11
2020	9.14	0.09	0.10	0.11
2021	7.20	0.09	0.11	0.11

Figures

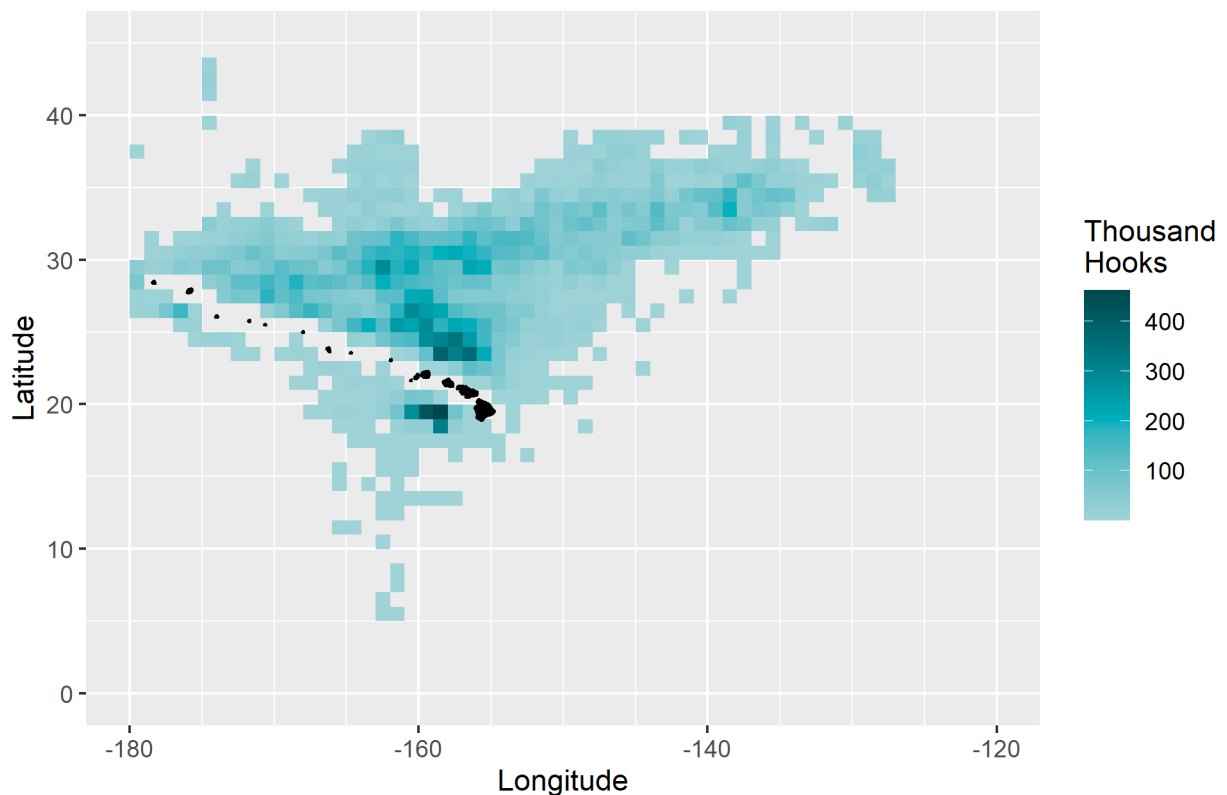


Figure 1. Total shallow-set fishing effort, in thousand hooks, aggregated from 1995–2021. Grid cells with fewer than 3 vessels have been excluded from the plot for confidentiality.

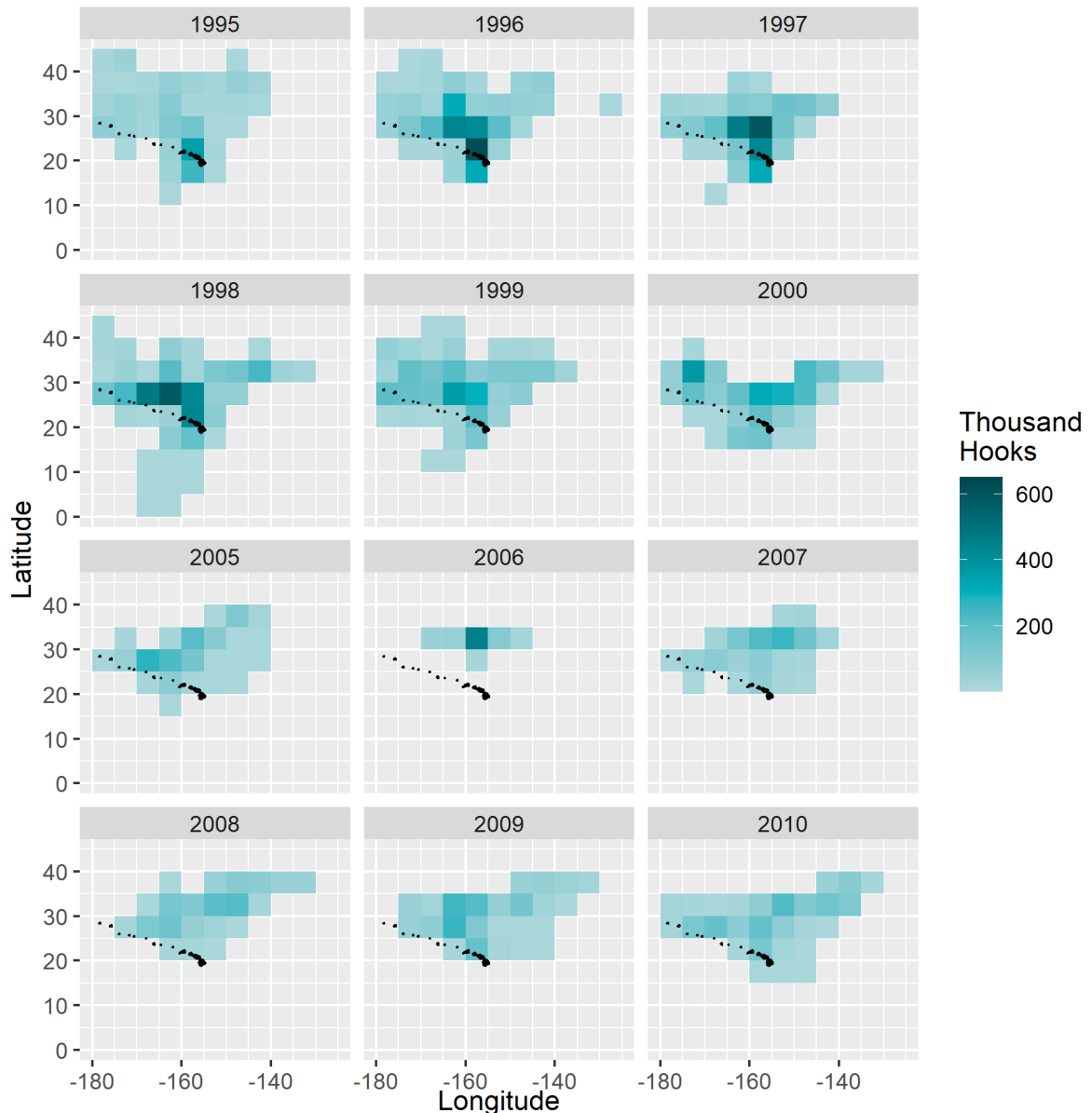


Figure 2. Shallow-set effort by year and $5 \times 5^\circ$ grid cells, in thousand hooks, 1995–2010. Grid cells with fewer than 3 vessels have been excluded from the plot for confidentiality.

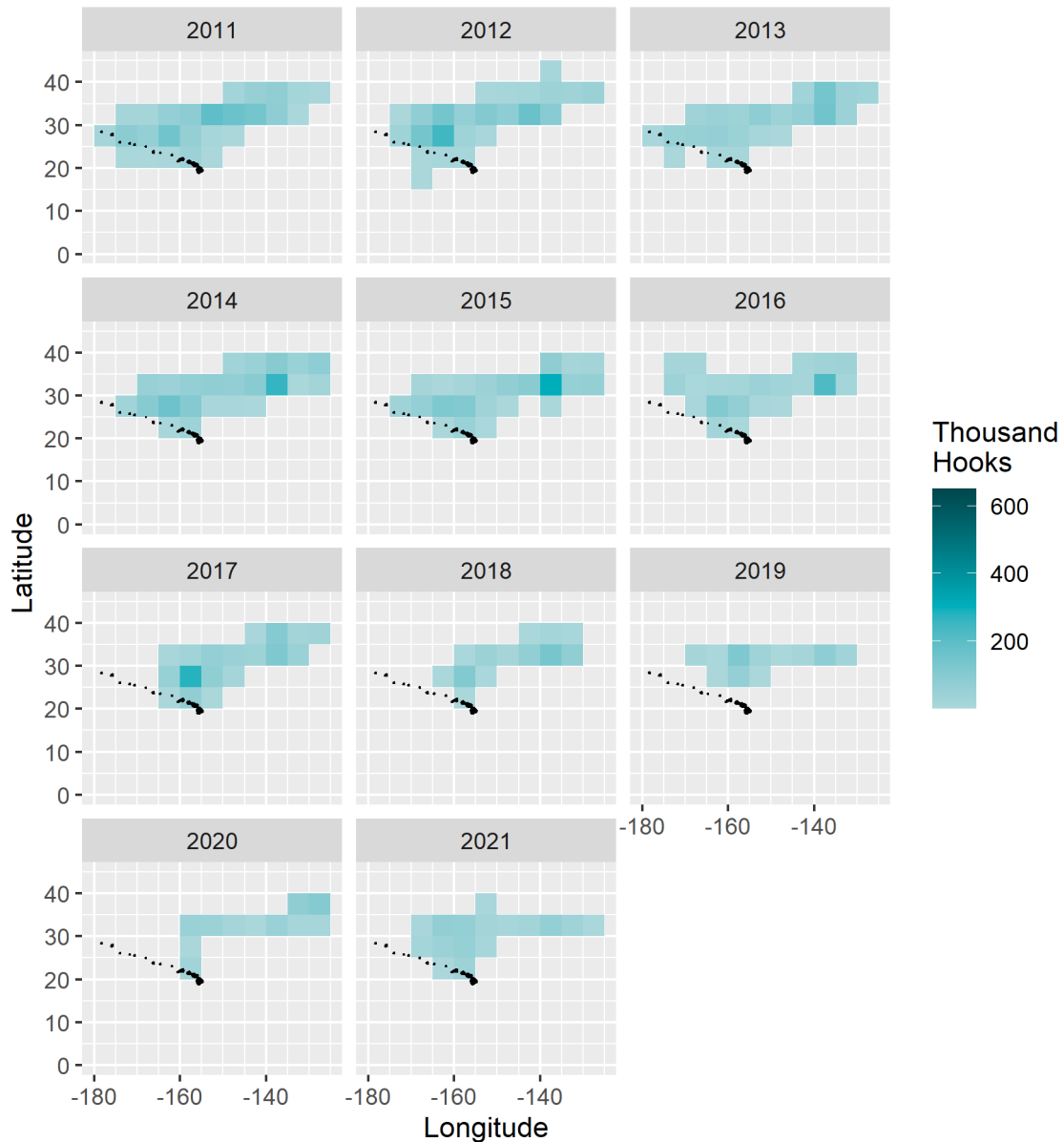


Figure 3. Shallow-set effort by year and $5 \times 5^\circ$ grid cells, in thousand hooks, 2011–2021. Grid cells with fewer than 3 vessels have been excluded from the plot for confidentiality.

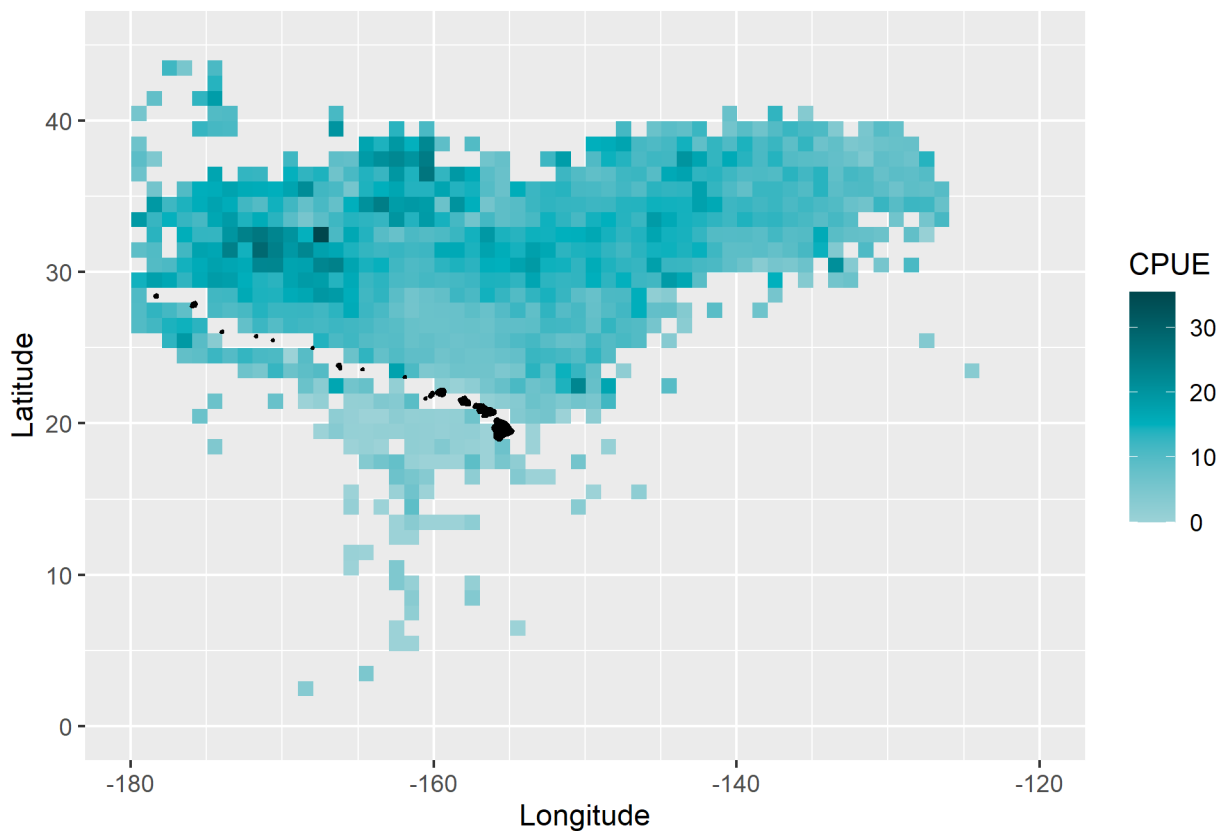


Figure 4. Total shallow-set nominal CPUE by $1 \times 1^\circ$ grid cells, in number per 1000 hooks, 1995–2021. Grid cells with fewer than 3 vessels have been excluded from the plot for confidentiality.

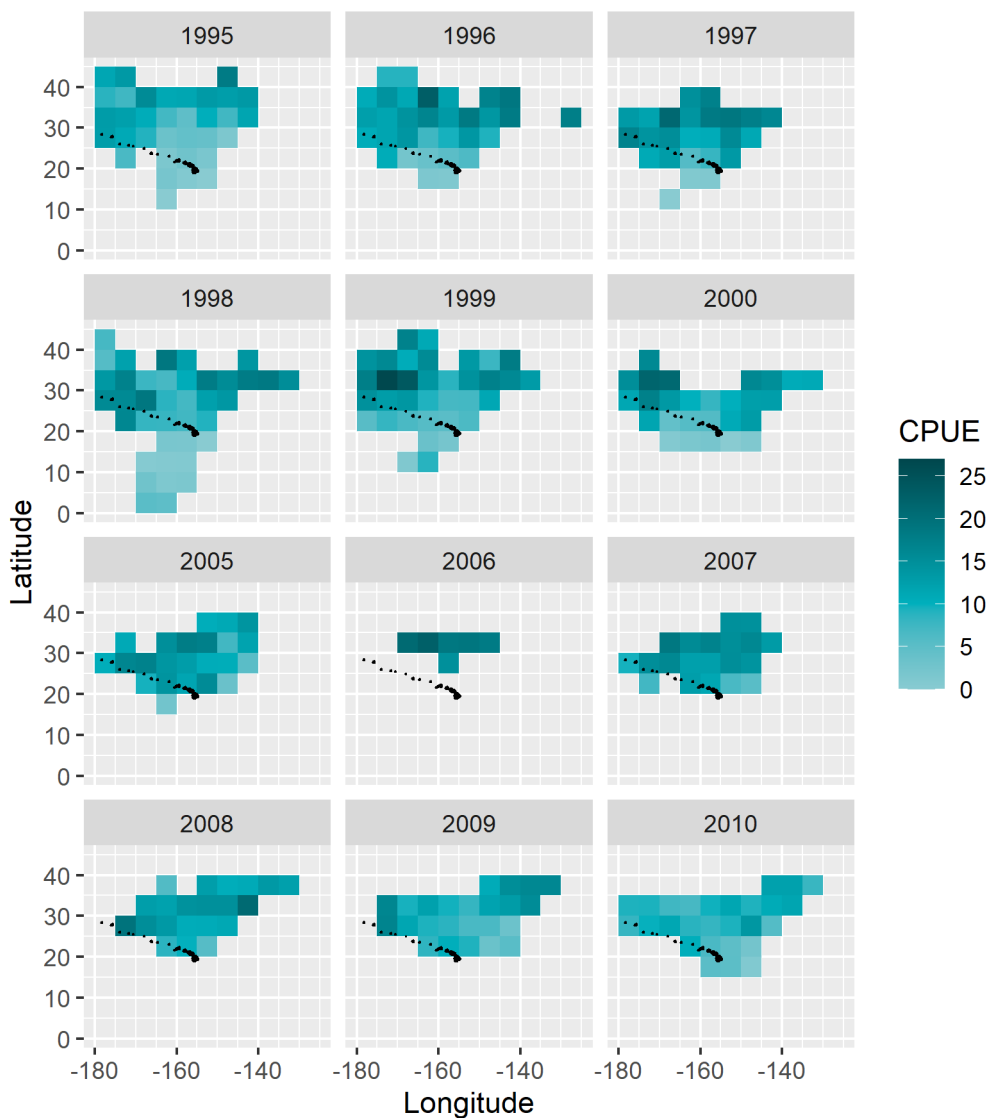


Figure 5. Shallow-set nominal CPUE by year and $5 \times 5^\circ$ grid cells, in number per 1000 hooks, 1995–2010. Grid cells with fewer than 3 vessels have been excluded from the plot for confidentiality.

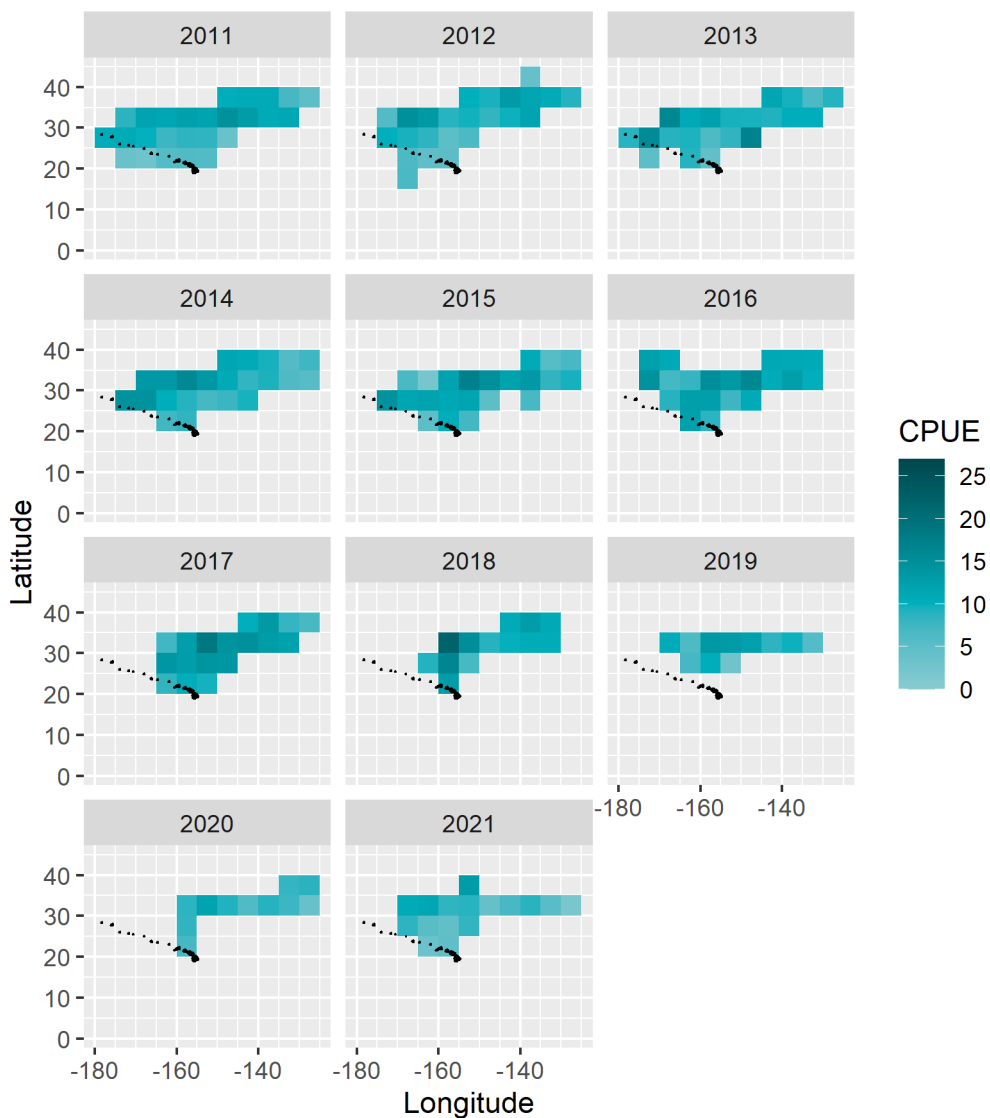


Figure 6. Shallow-set nominal CPUE by year and $5 \times 5^\circ$ grid cells, in number per 1000 hooks, 2011–2021. Grid cells with fewer than 3 vessels have been excluded from the plot for confidentiality.

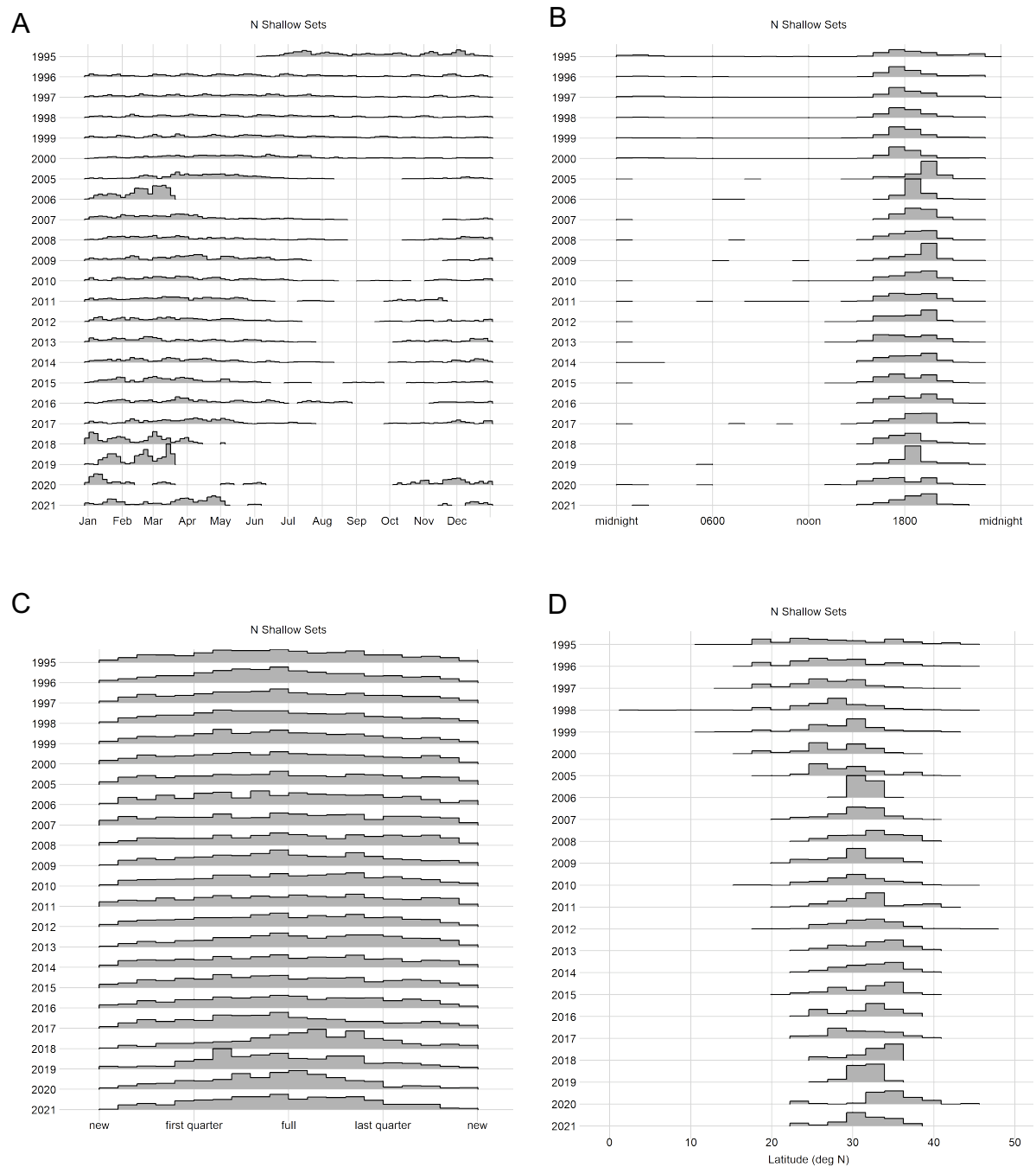


Figure 7. Relative frequency plots of shallow-sets per year by (A) time of year, (B) time of day, (C) moon phase, and (D) latitude. The y-axes are scaled so shaded area is equal for each year within each covariate.

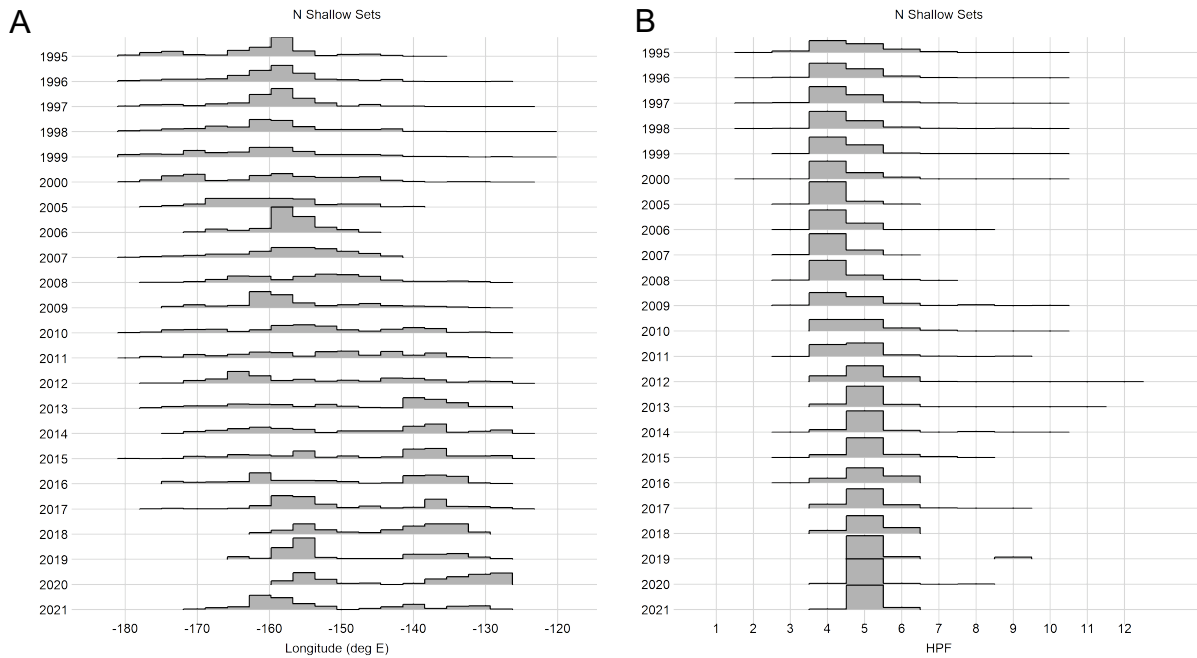


Figure 8. Relative frequency plots of shallow-sets per year by (A) longitude and (B) hooks per float (HPF). The y-axes are scaled so shaded area is equal for each year within each covariate.

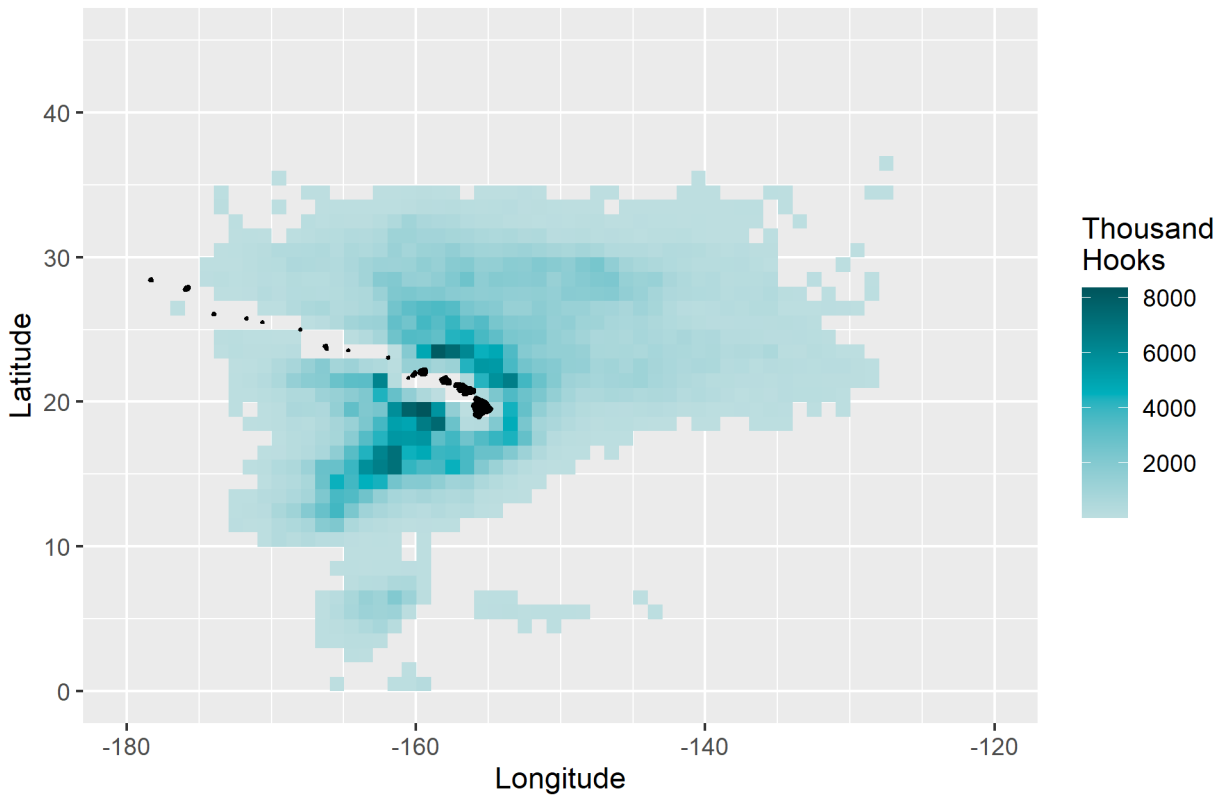


Figure 9. Total deep-set effort by $1 \times 1^\circ$ grid cells, in thousand hooks, 1995–2021. Grid cells with fewer than 3 vessels have been excluded from the plot for confidentiality.

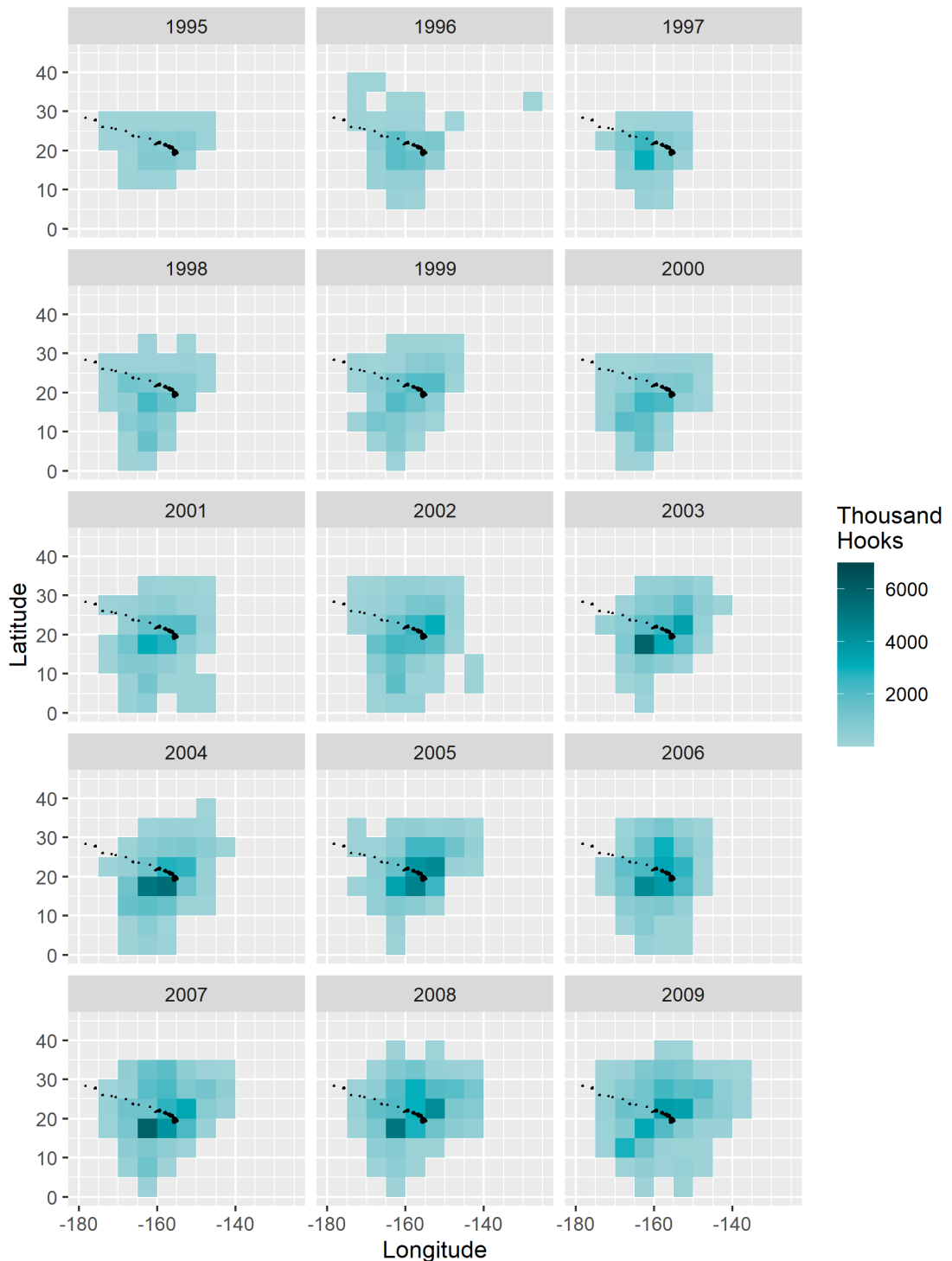


Figure 10. Deep-set effort by year and $5 \times 5^\circ$ grid cells, in thousand hooks, 1995–2009. Grid cells with fewer than 3 vessels have been excluded from the plot for confidentiality.

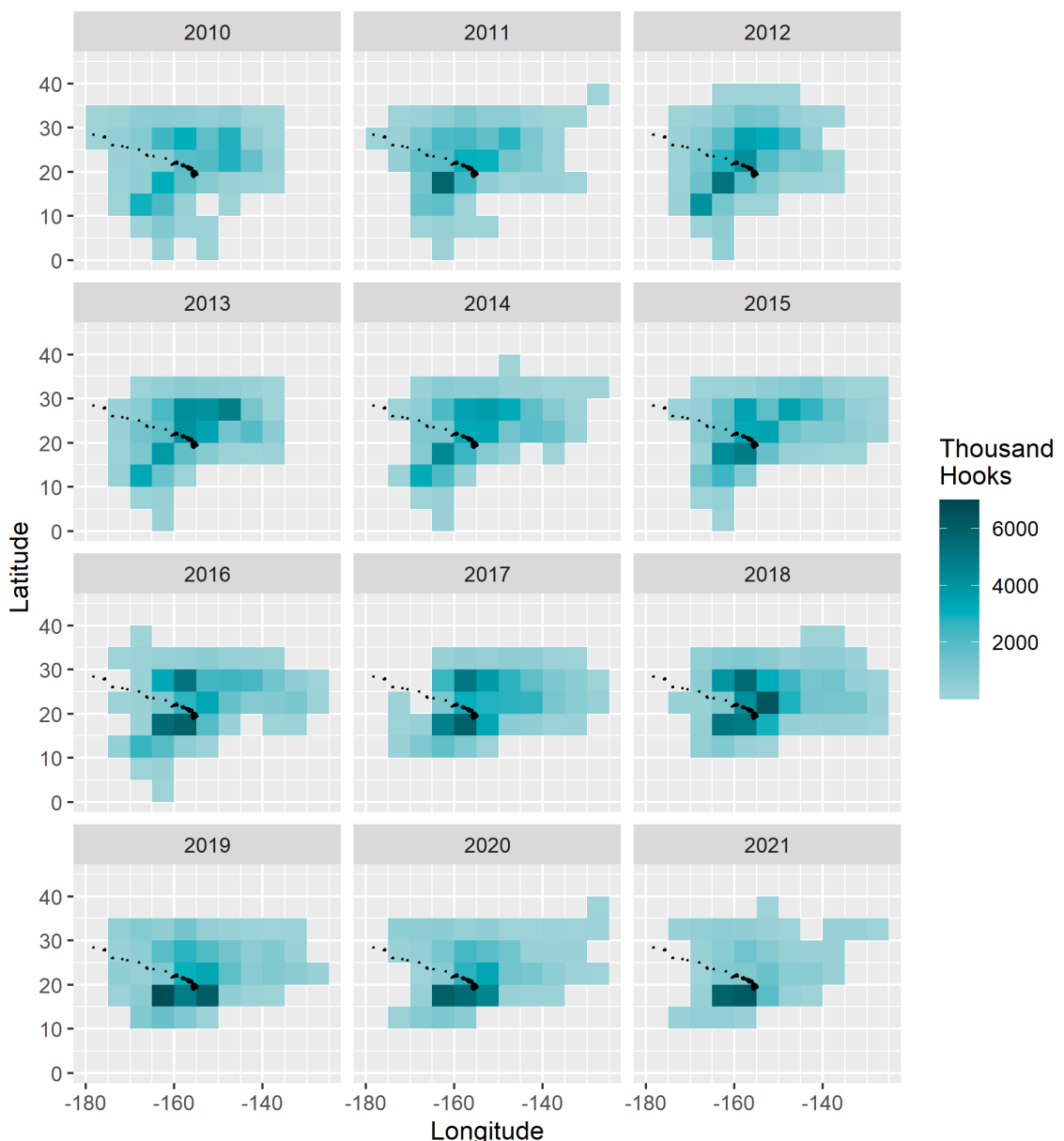


Figure 11. Deep-set effort by year and $5 \times 5^\circ$ grid cells, in thousand hooks, 2010–2021. Grid cells with fewer than 3 vessels have been excluded from the plot for confidentiality.

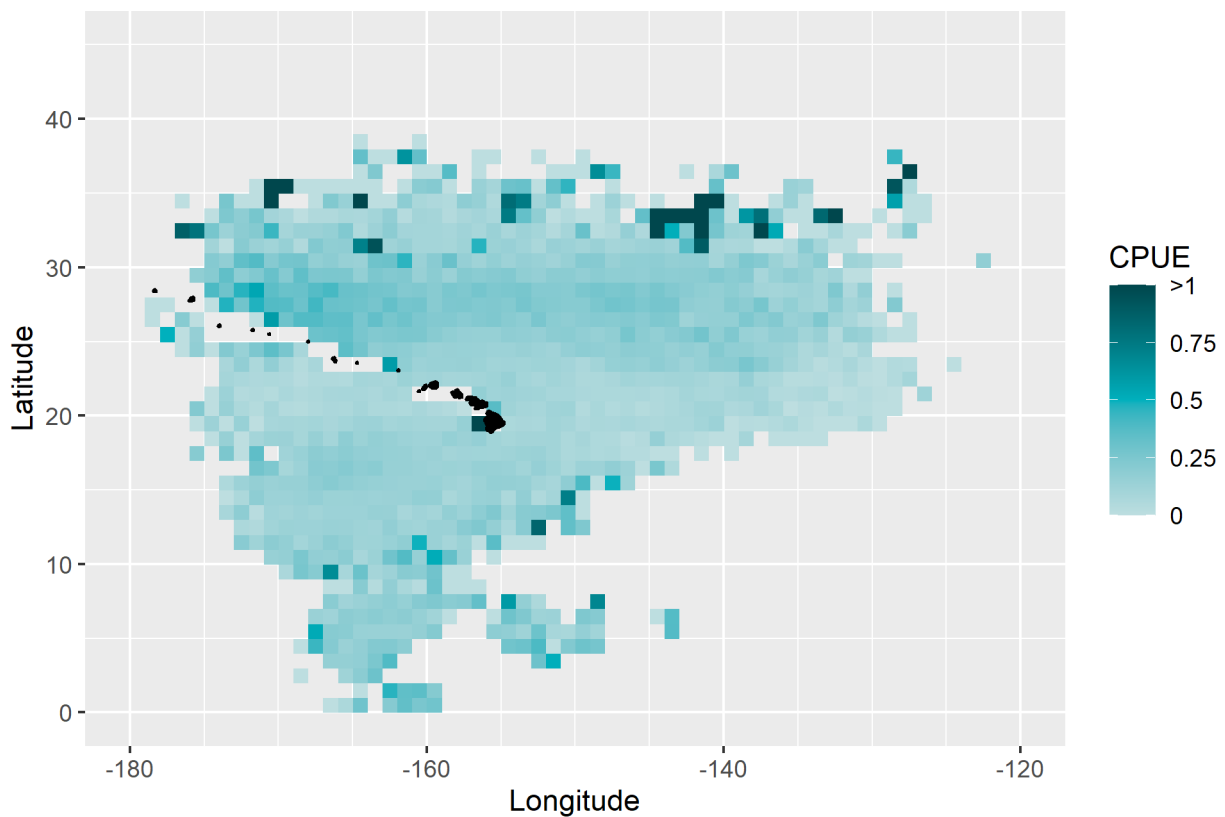


Figure 12. Total deep-set nominal CPUE by $1 \times 1^\circ$ grid cells, in number per 1000 hooks, 1995–2021. Grid cells with fewer than 3 vessels have been excluded from the plot for confidentiality.

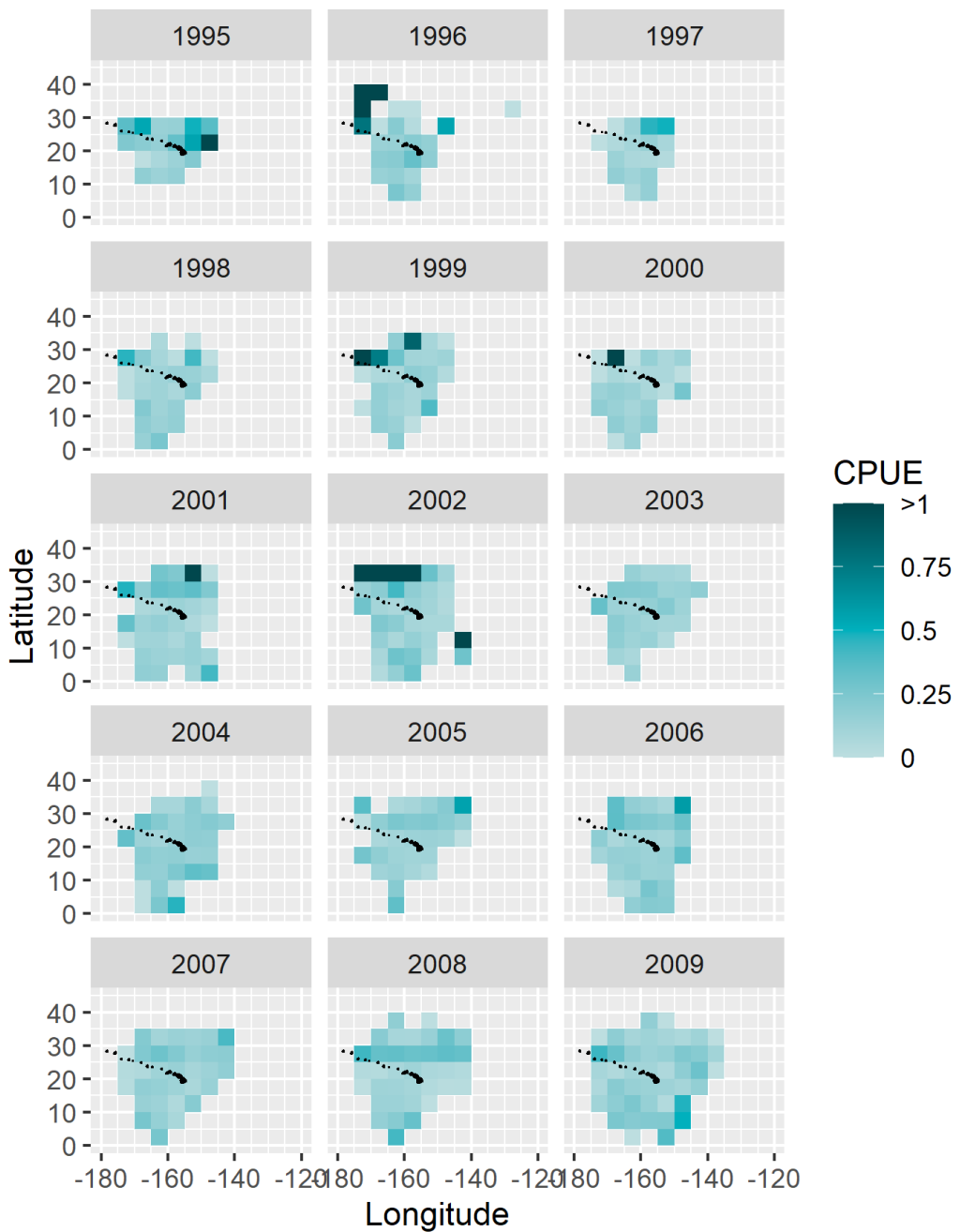


Figure 13. Deep-set nominal CPUE by year and $5 \times 5^\circ$ grid cells, in number per 1000 hooks, 1995–2009. Grid cells with fewer than 3 vessels have been excluded from the plot for confidentiality.

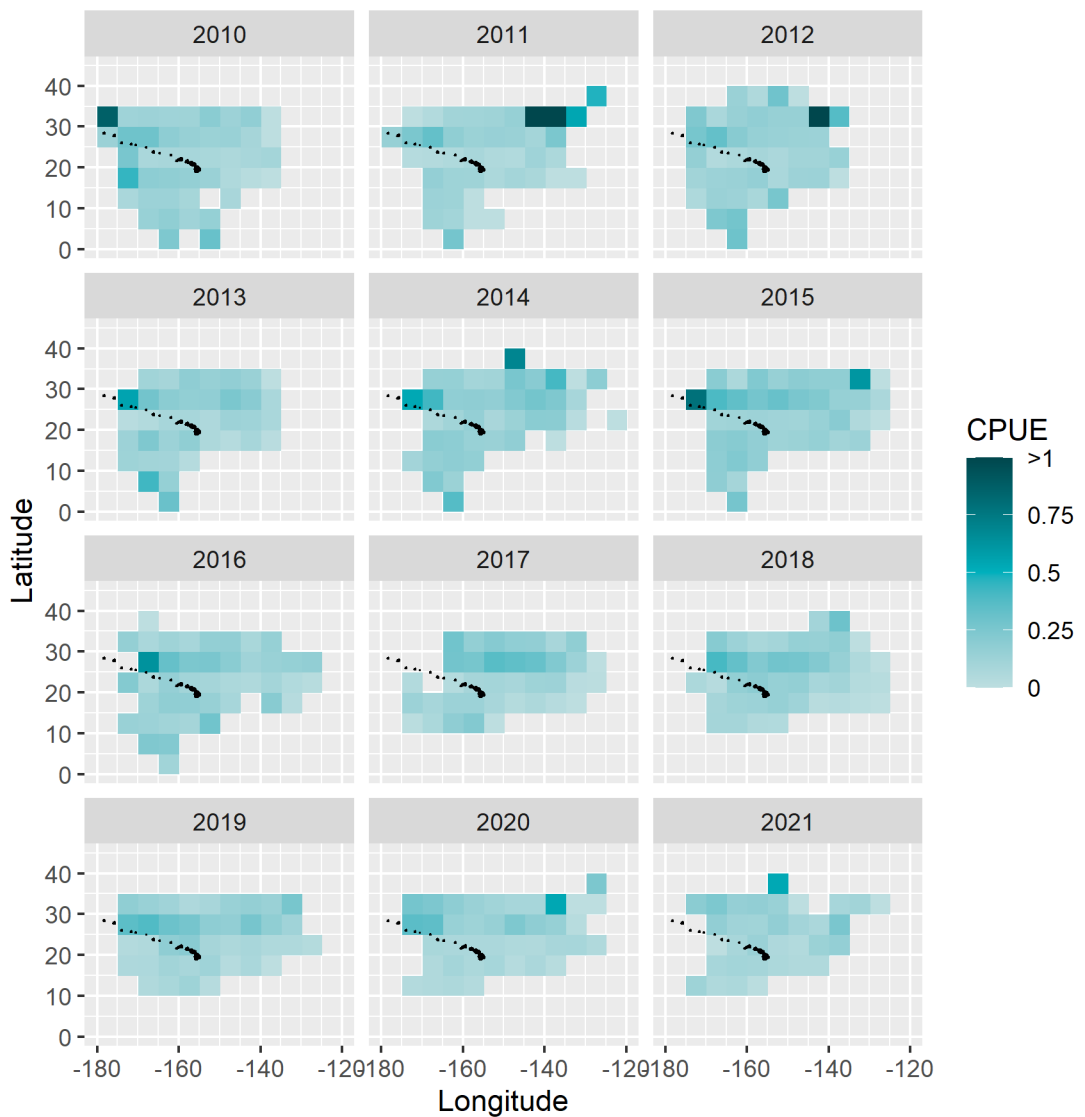


Figure 14. Deep-set nominal CPUE by year and $5 \times 5^\circ$ grid cells, in number per 1000 hooks, 2010–2021. Grid cells with fewer than 3 vessels have been excluded from the plot for confidentiality.

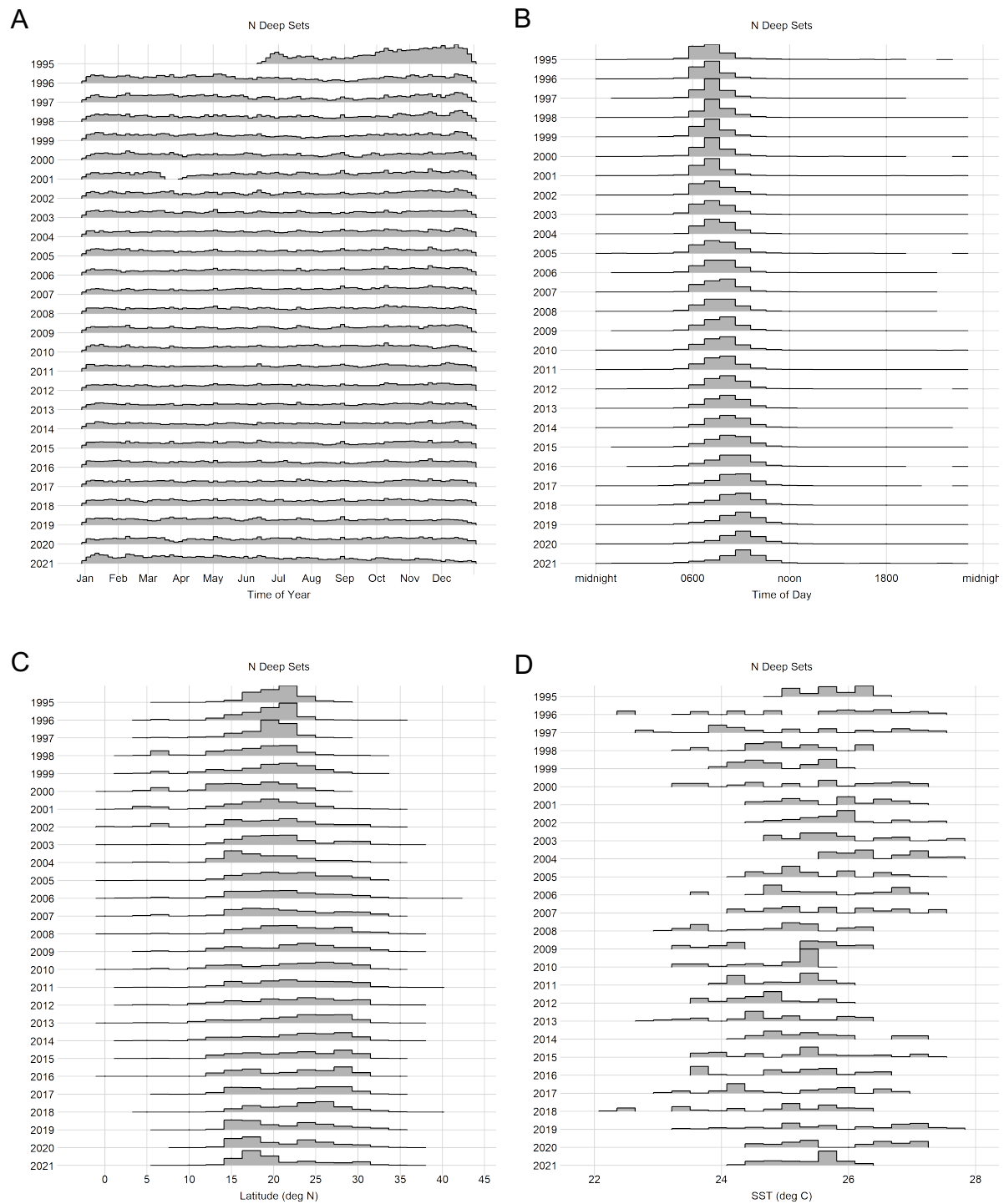


Figure 15. Relative frequency plots of deep-sets per year by (A) time of year, (B) time of day, (C) latitude, and (D) sea surface temperature (SST). The y-axes are scaled so shaded area is equal for each year within each covariate.

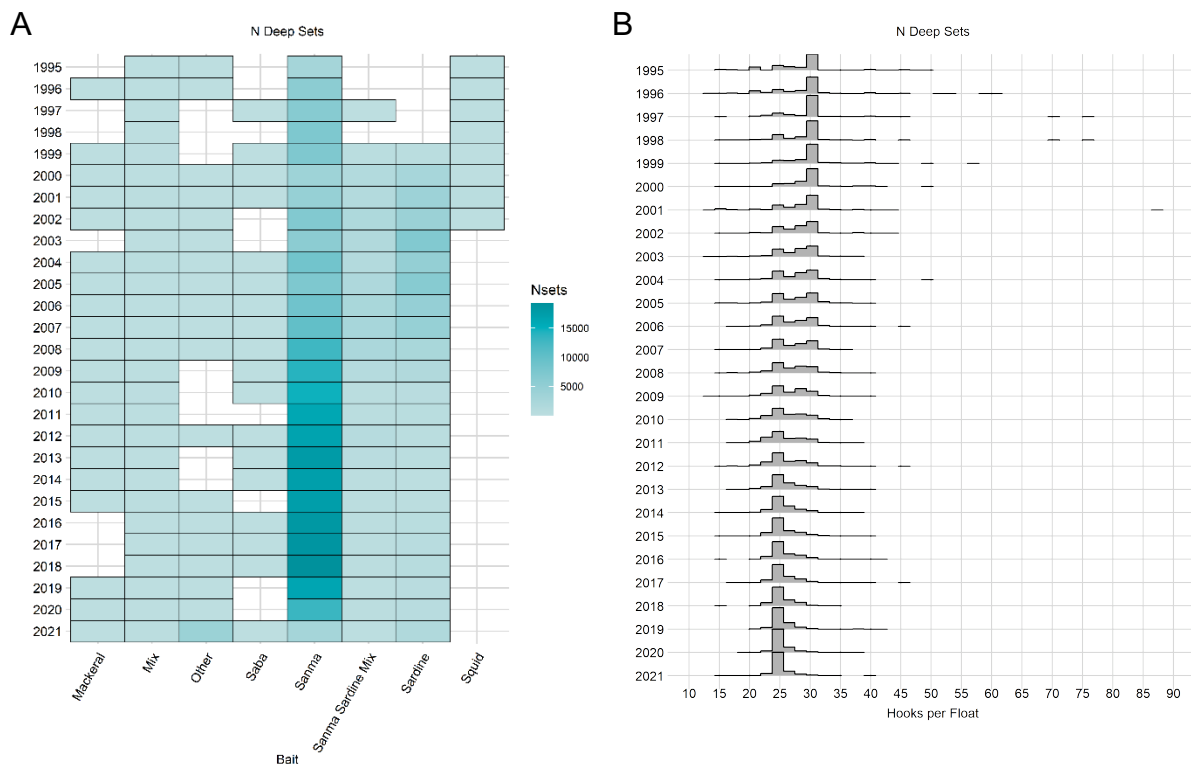


Figure 16. Relative frequency plots of deep-sets per year by (A) bait type and (B) hooks per float (HPF). The y-axes are scaled so shaded area is equal for each year within each covariate.

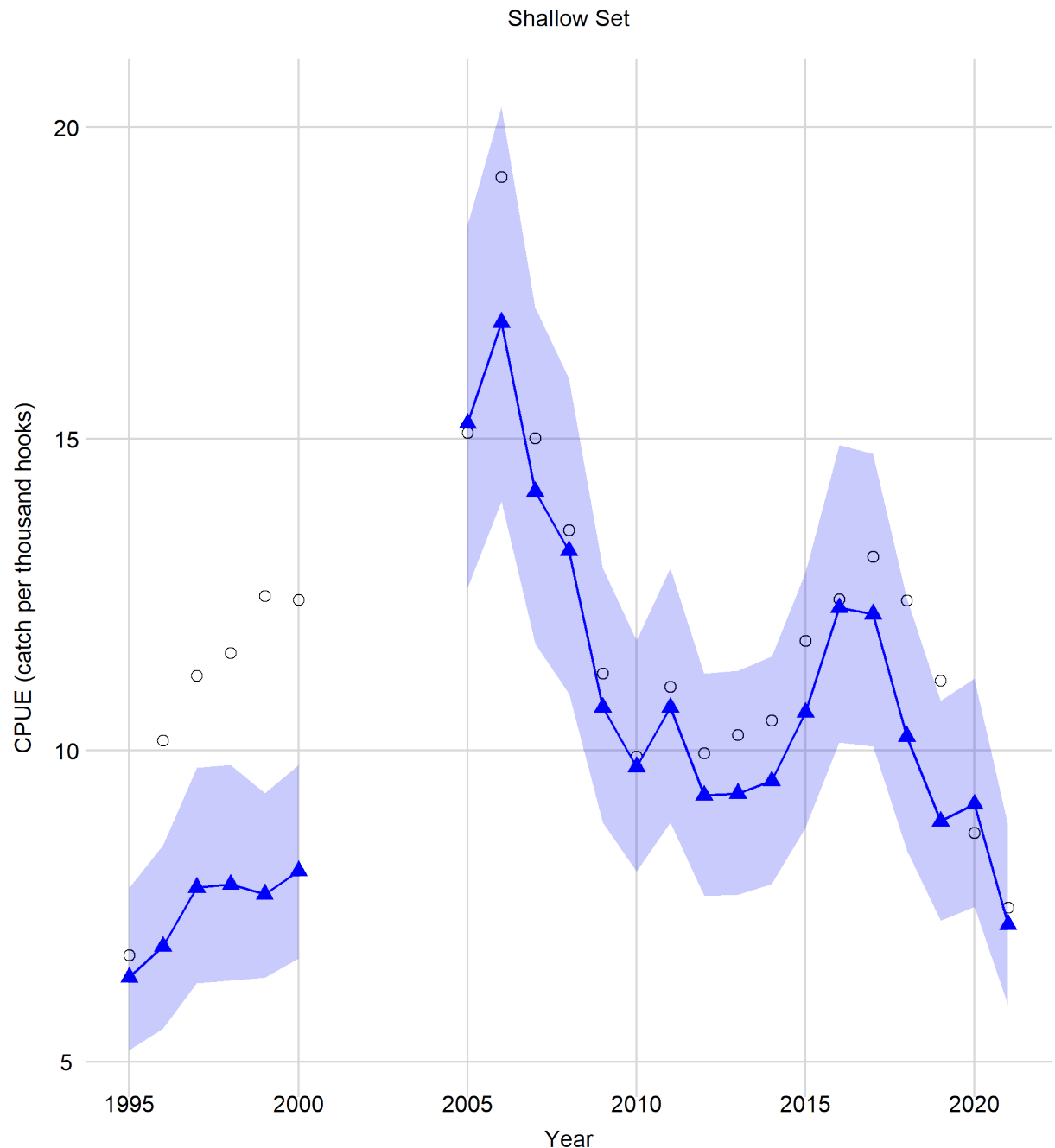


Figure 17. Shallow-set annual standardized CPUE (triangles) with 95% confidence intervals (shaded) for the 1995–2000 and 2005–2021 time-series. Open symbols are nominal CPUE.

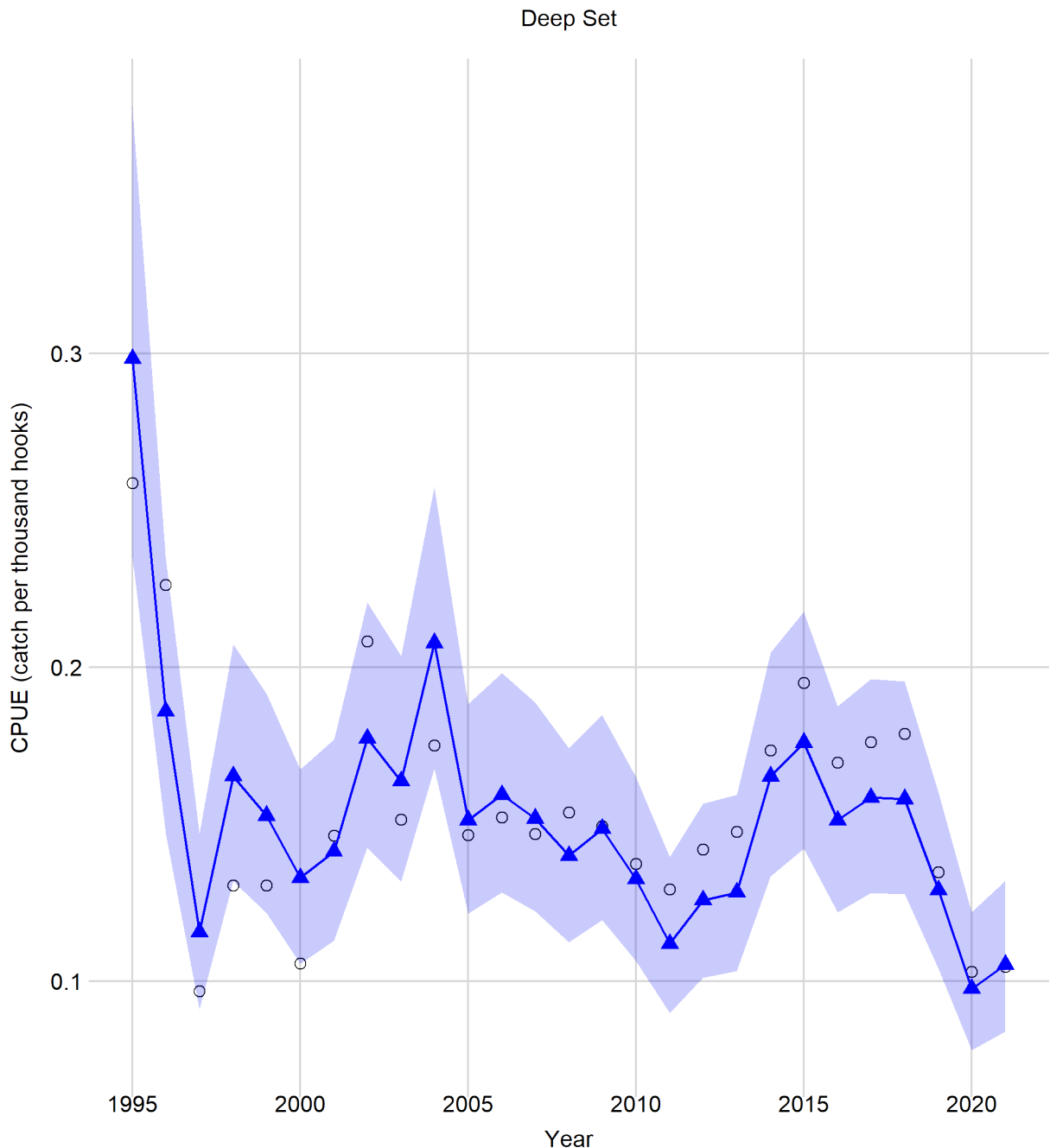


Figure 18. Deep-set annual standardized CPUE (triangles) with 95% confidence intervals (shaded) for 1995–2021. Open symbols are nominal CPUE.

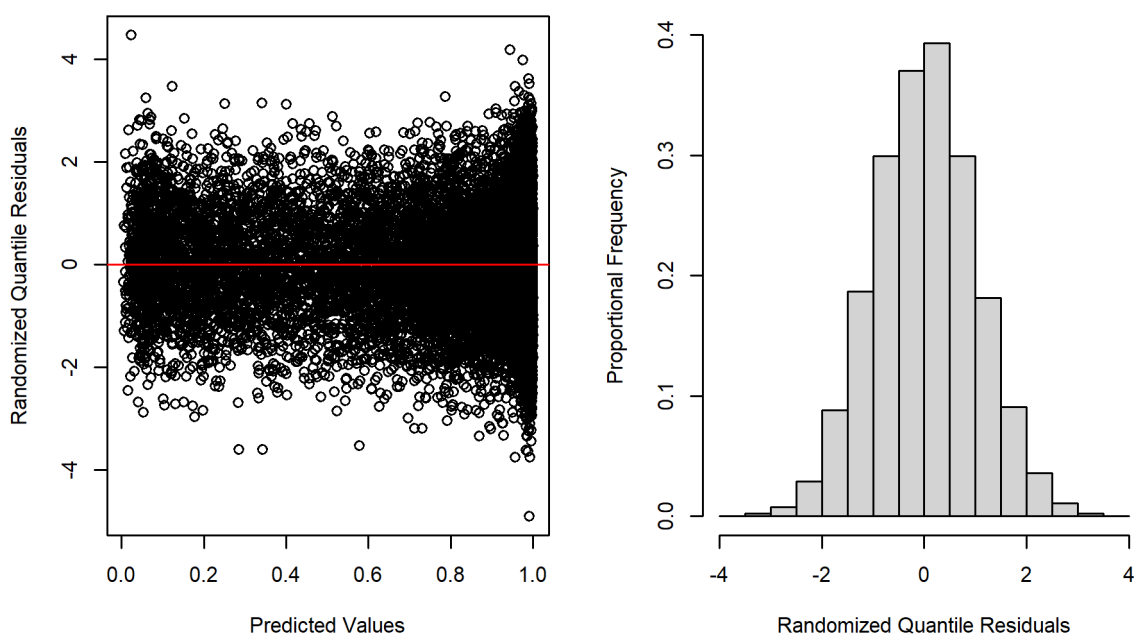


Figure 19. Plots of randomized quantile residuals for the shallow-set 1995–2000 presence/absence GAMMs.

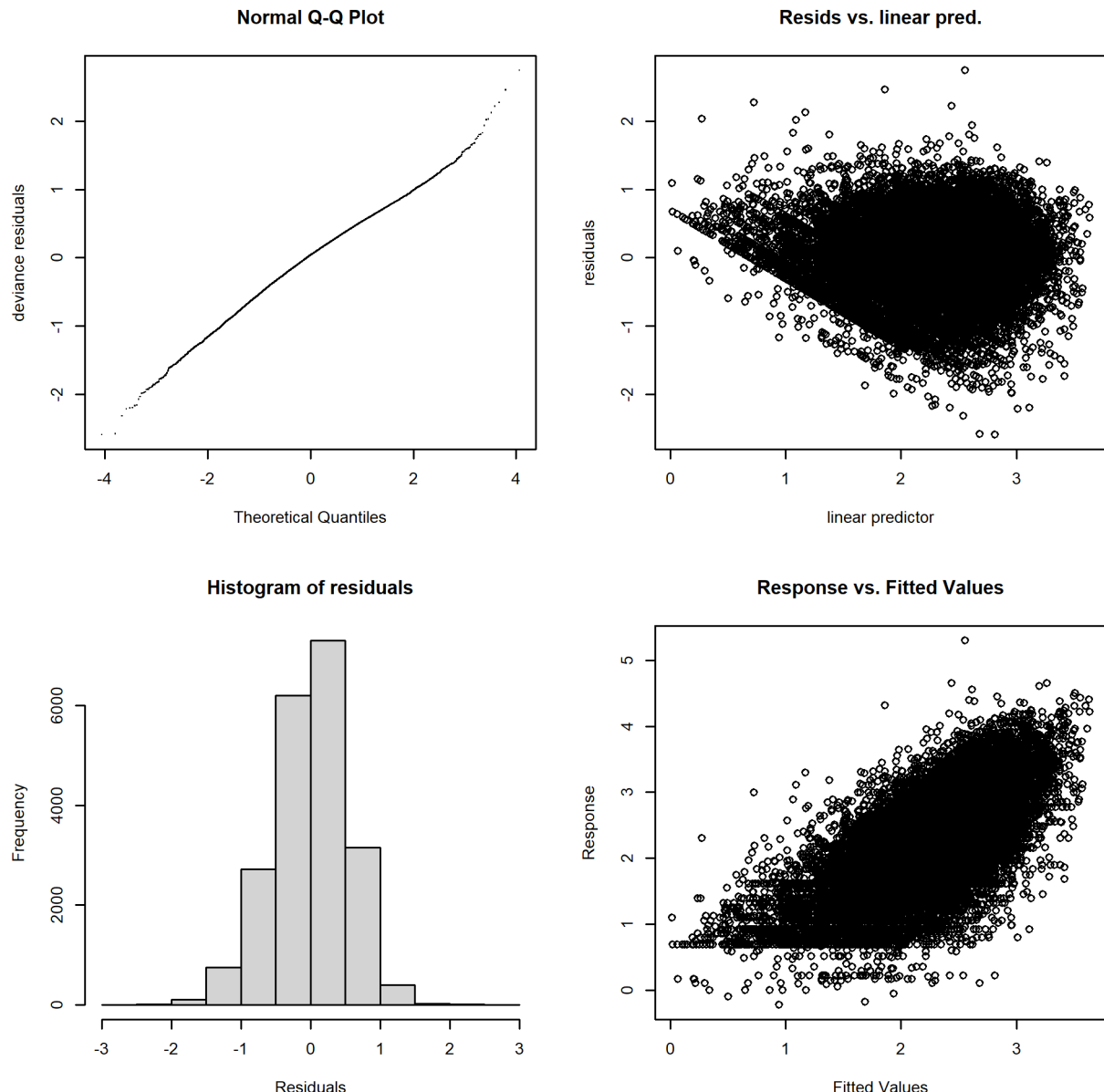


Figure 20. Shallow-set 1995–2000 positive process GAMM model diagnostics. Response is shown on the log scale.

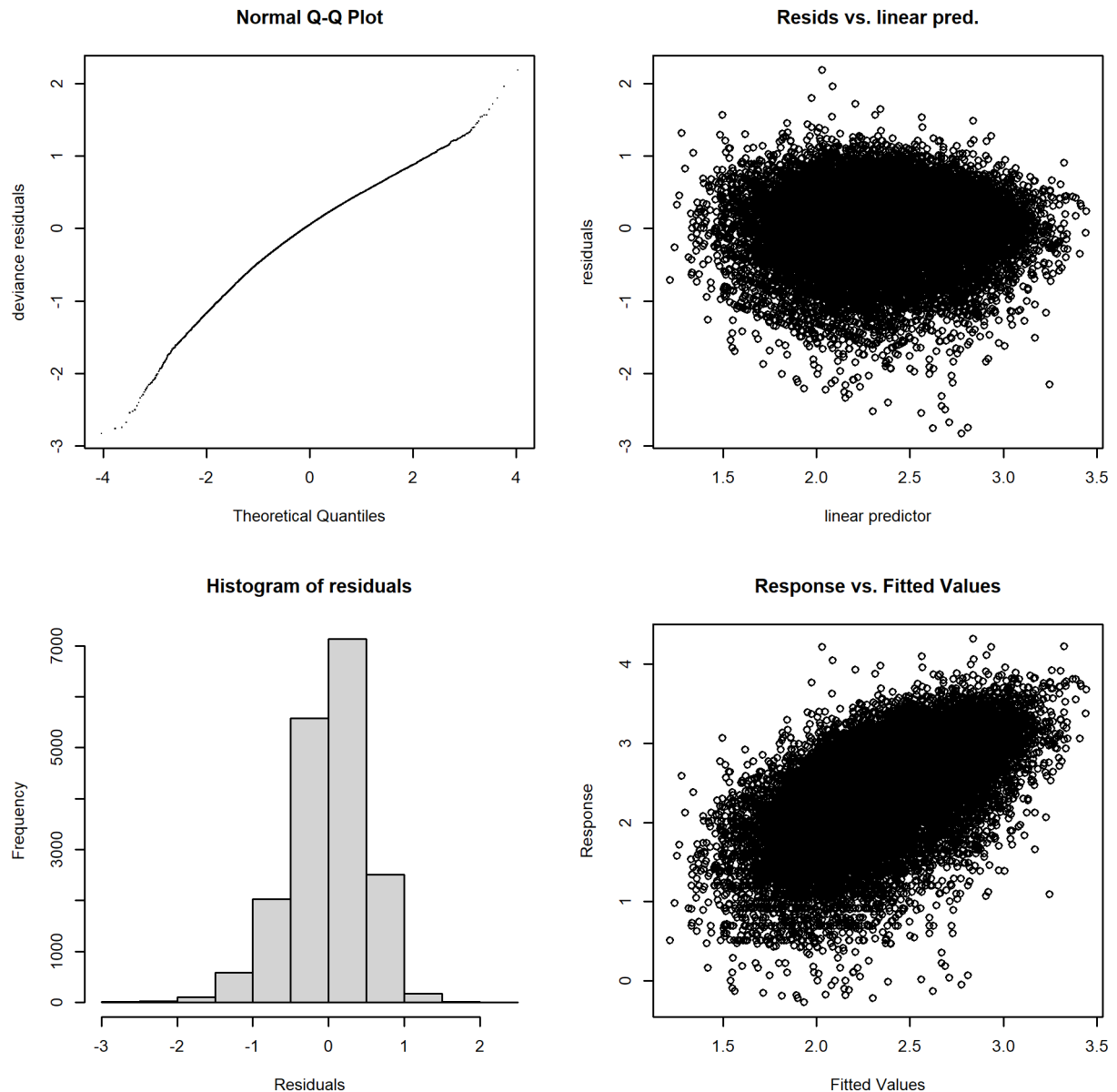


Figure 21. Shallow-set 2005–2021 positive process GAMM model diagnostics. Response is shown on the log scale.

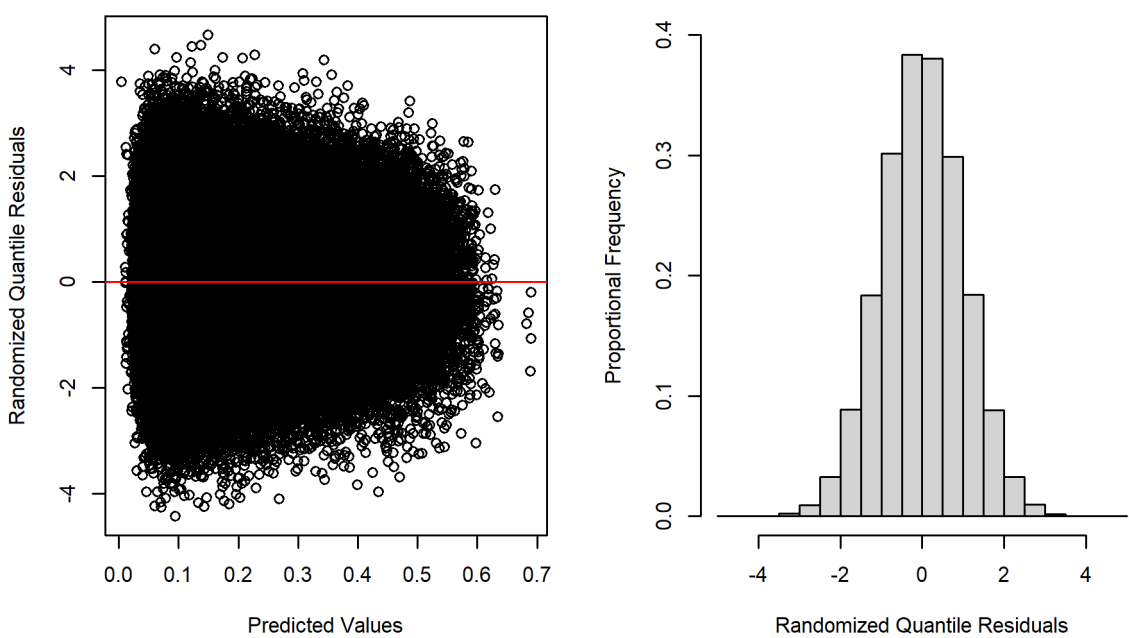


Figure 22. Deep-set presence/absence GAMM model diagnostics.

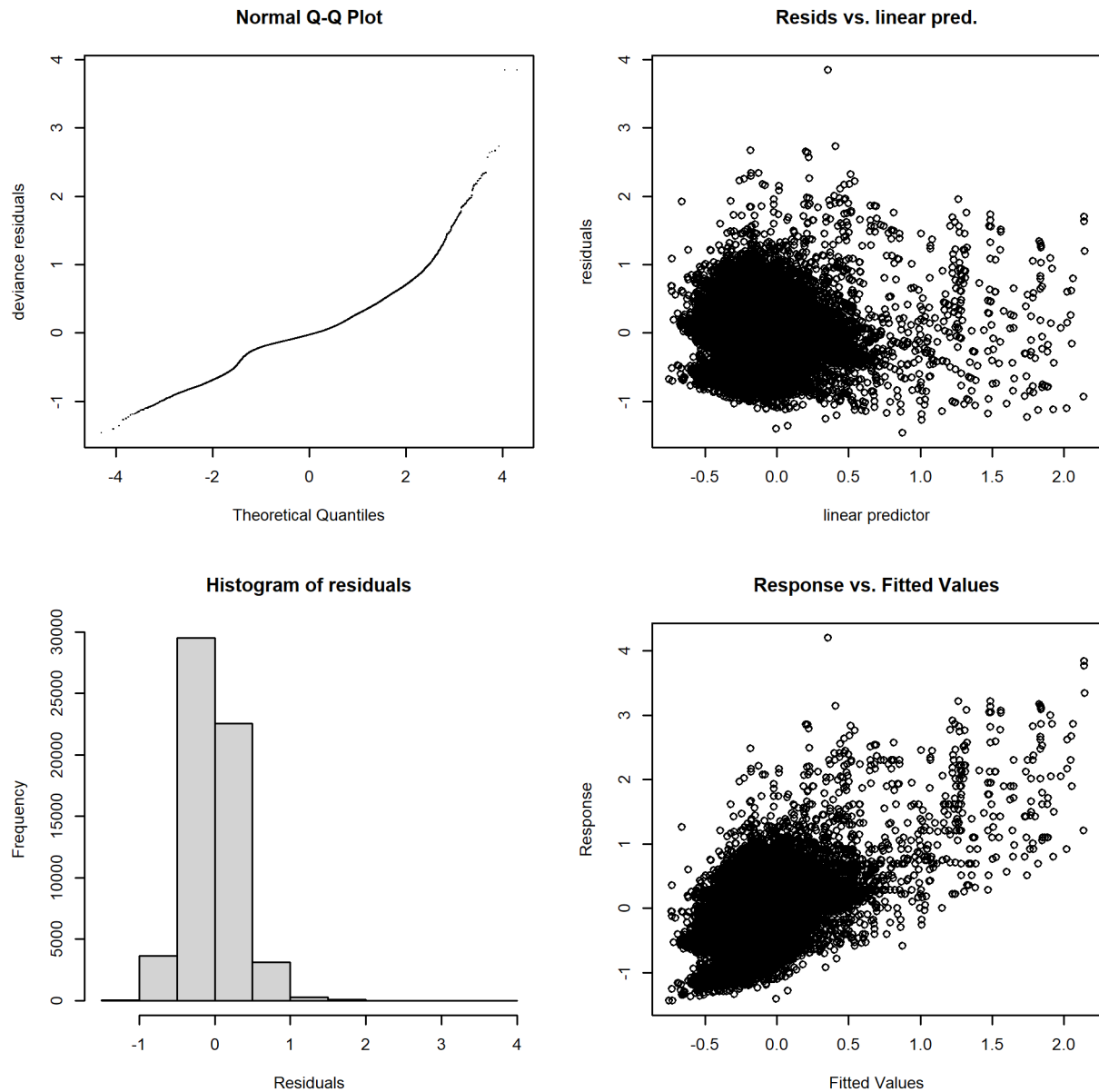


Figure 23. Deep-set positive process GAMM model diagnostics. Response is shown on the log scale.

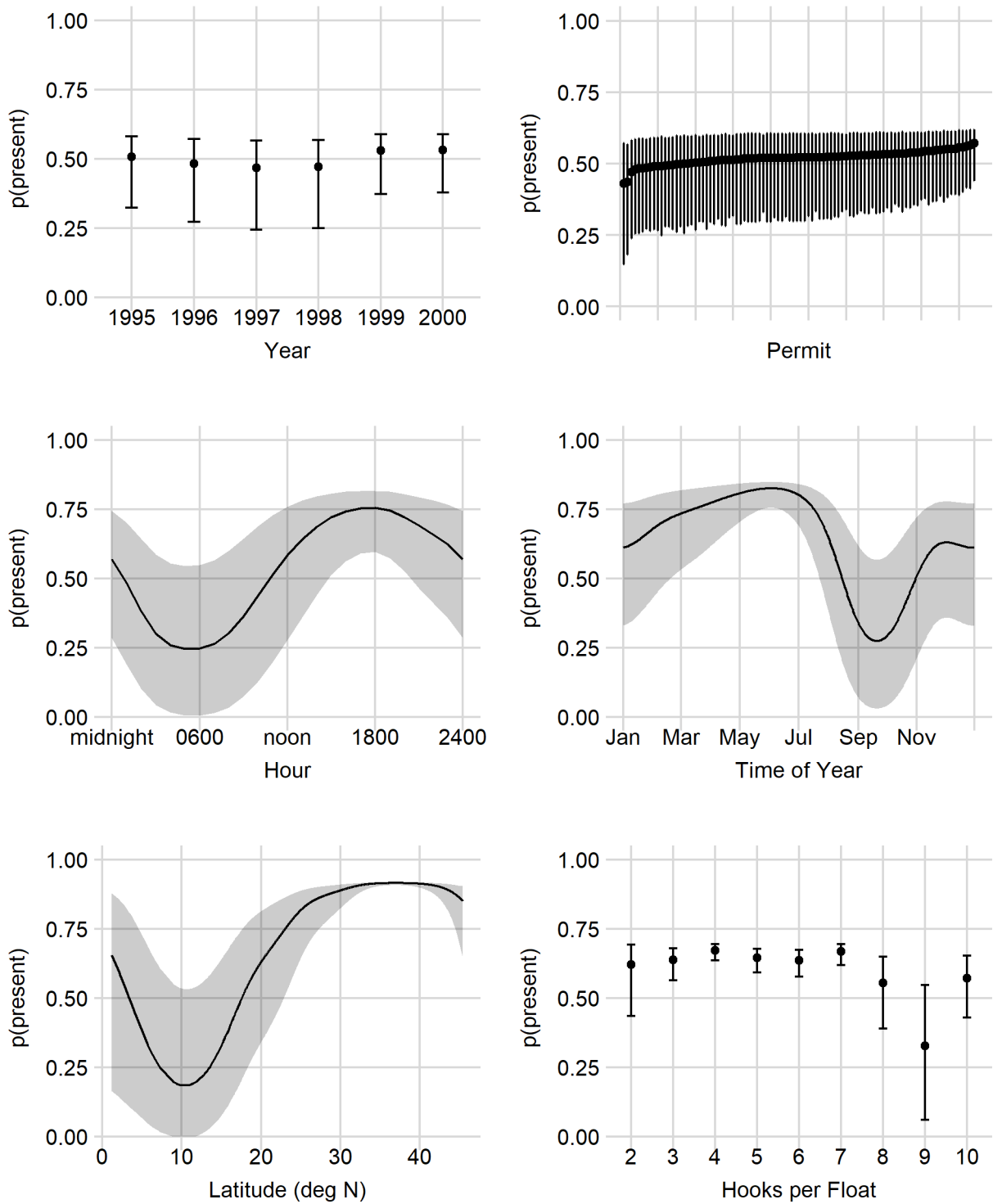


Figure 24. Shallow-set 1995–2000 presence/absence marginal effects of each GAMM covariate. Error bars and shaded areas represent 95% confidence intervals.

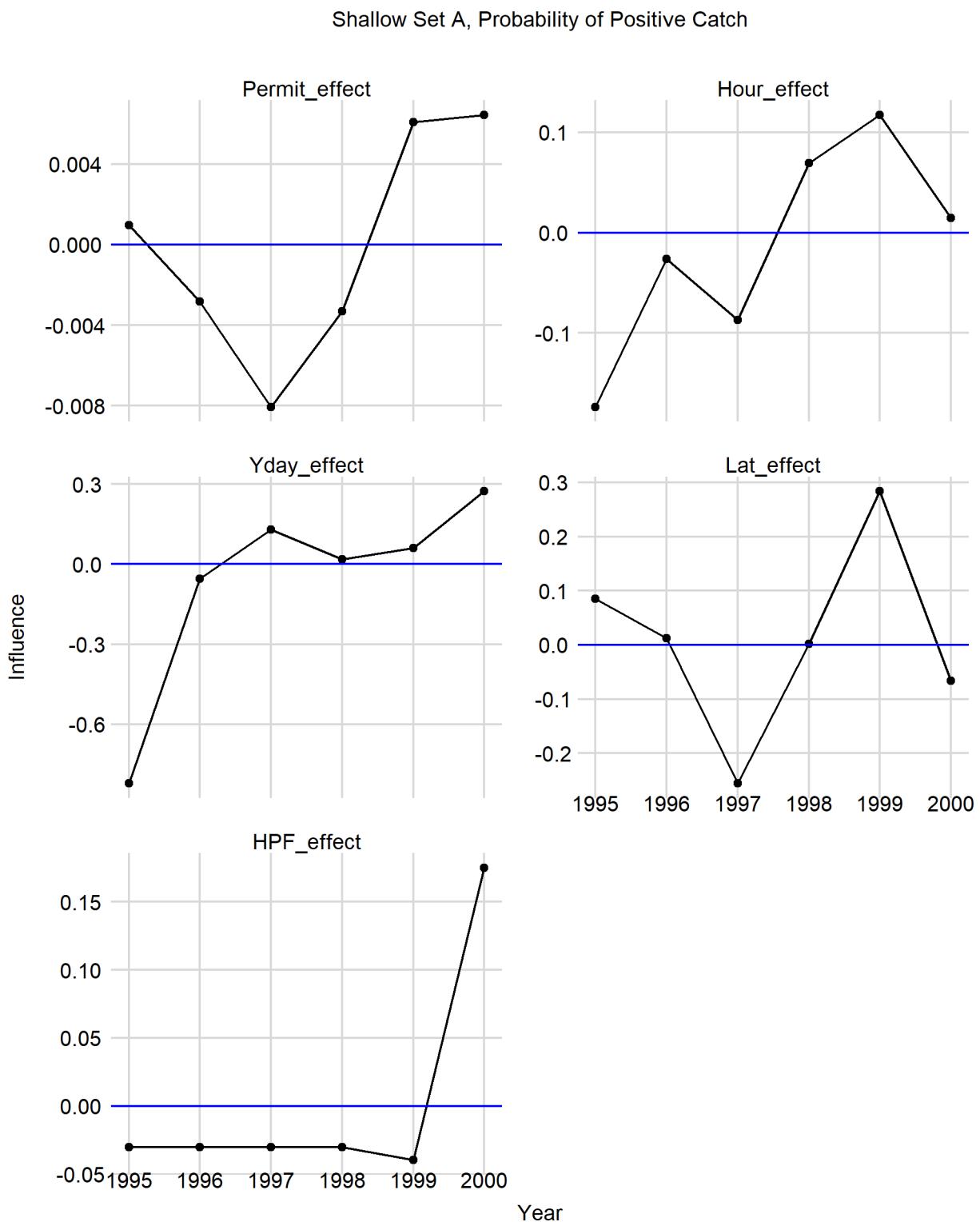


Figure 25. Shallow-set 1995–2000 presence/absence influence over time of each GAMM covariate.

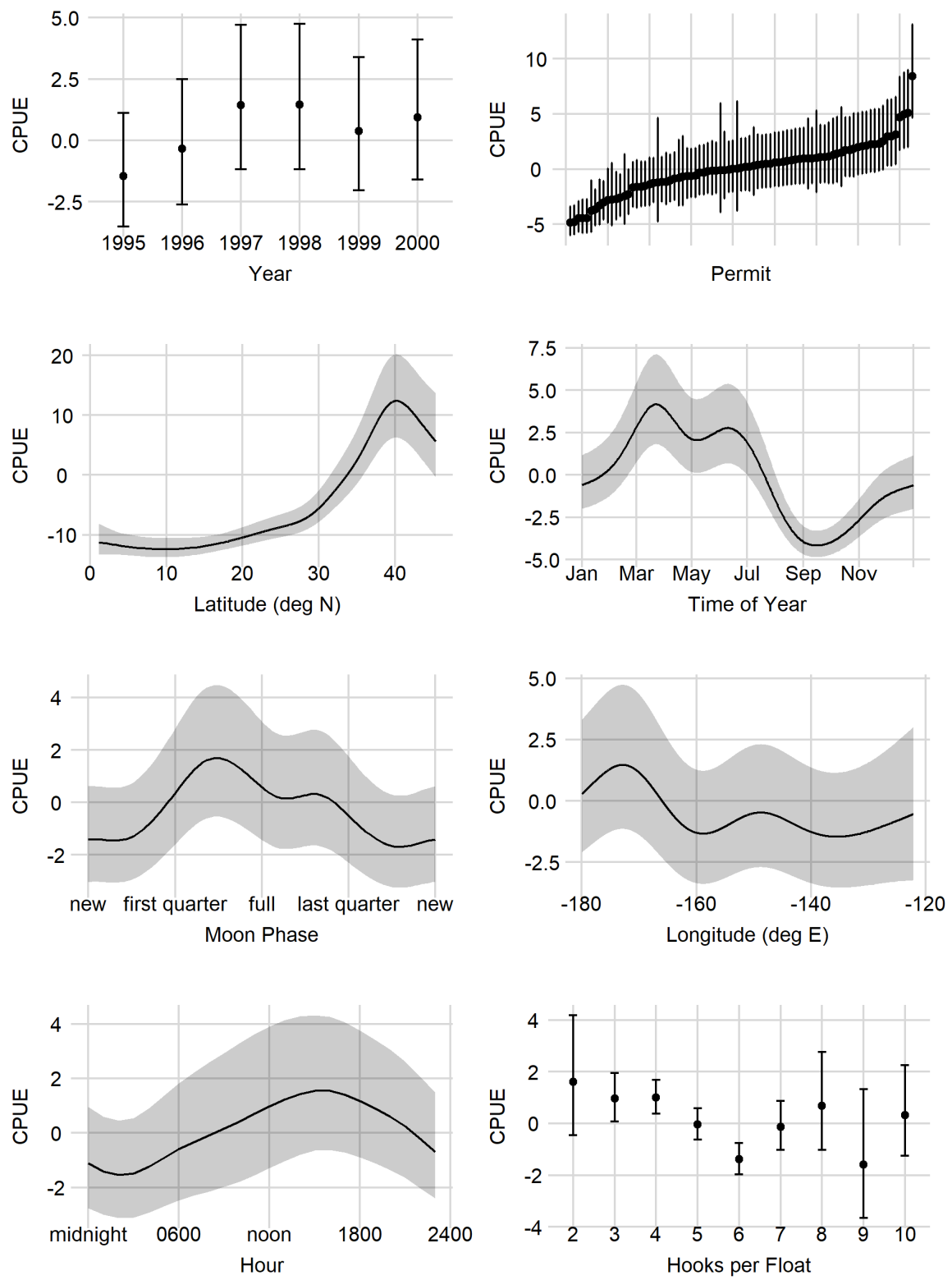


Figure 26. Shallow-set 1995–2000 positive process marginal effects of each GAMM covariate. Error bars and shaded areas represent 95% confidence intervals.

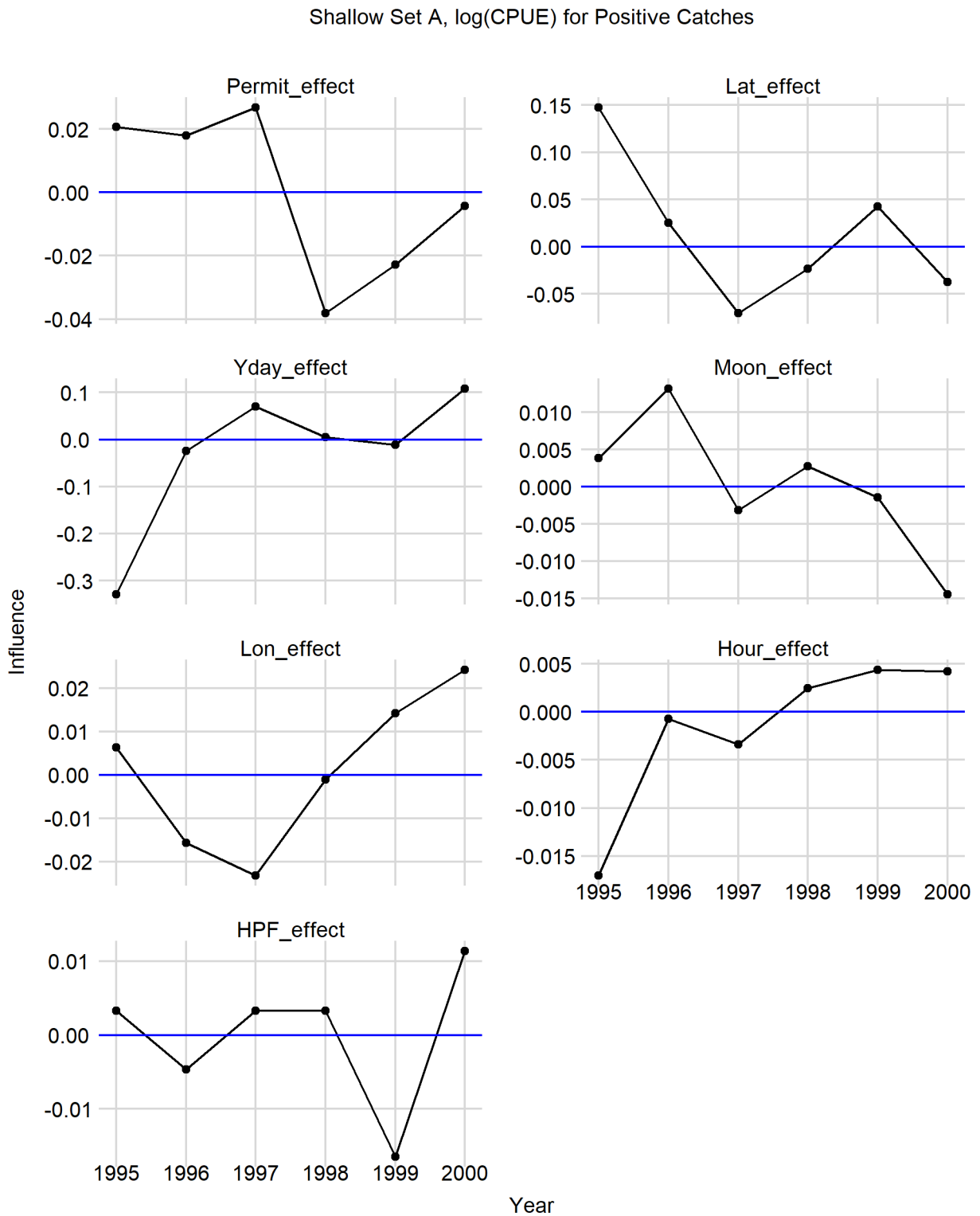


Figure 27. Shallow-set 1995–2000 positive process influence over time of each GAMM covariate.

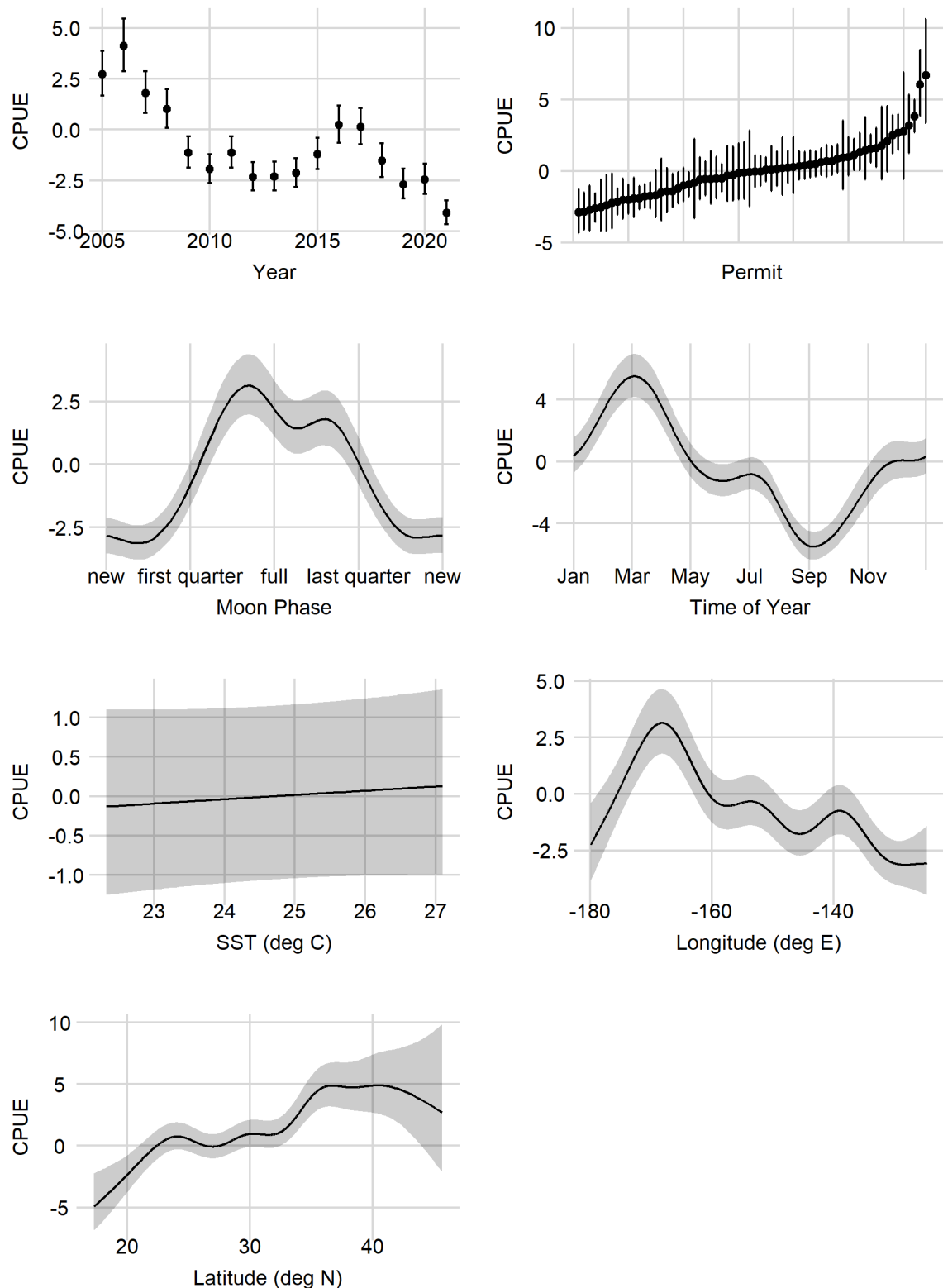


Figure 28. Shallow-set 2005–2021 positive process marginal effects of each GAMM covariate. Error bars and shaded areas represent 95% confidence intervals.

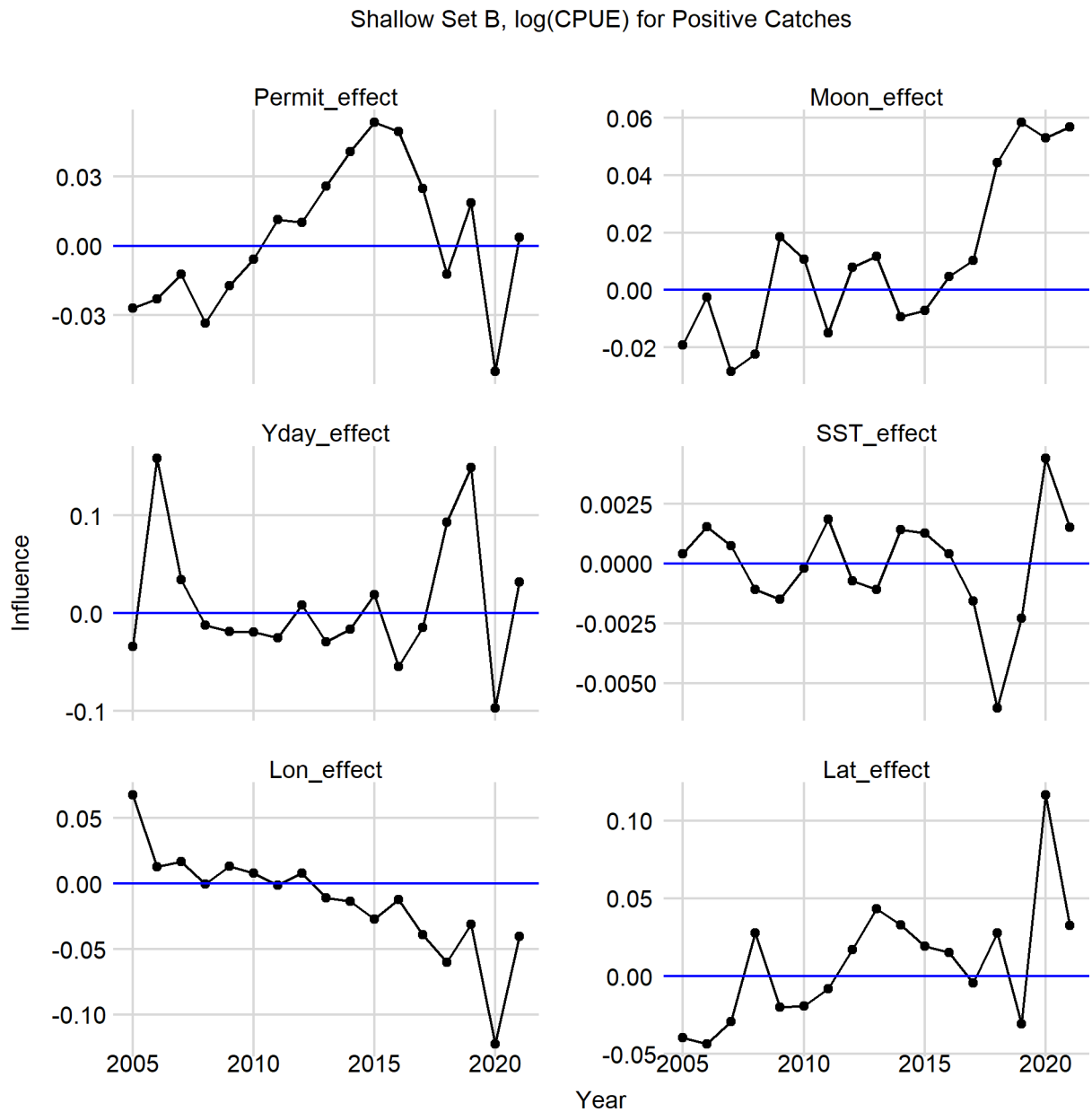


Figure 29. Shallow-set 2005–2021 positive process influence over time of each GAMM covariate.

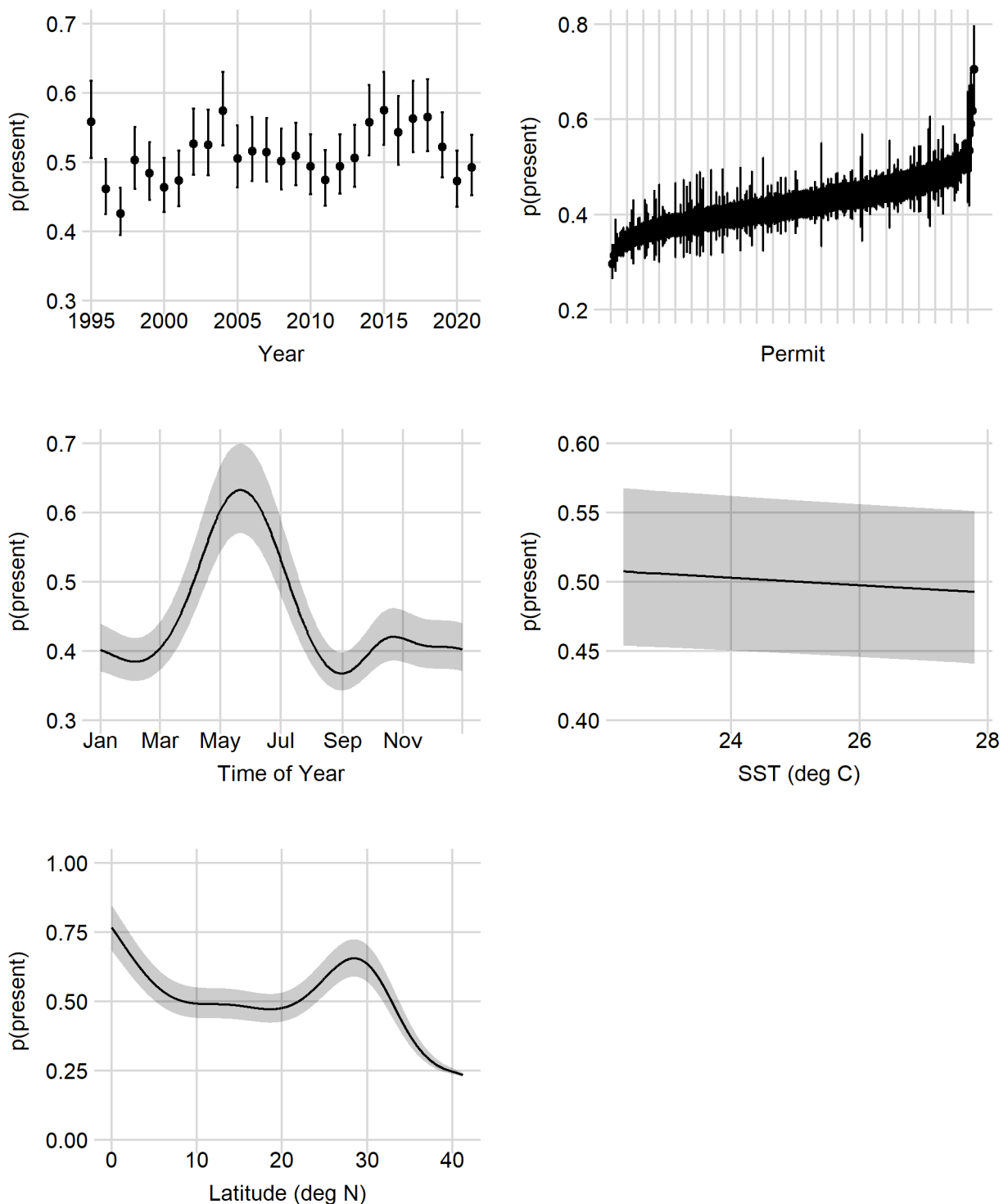


Figure 30. Deep-set 1995–2021 presence/absence marginal effects of each GAMM covariate. Error bars and shaded areas represent 95% confidence intervals.

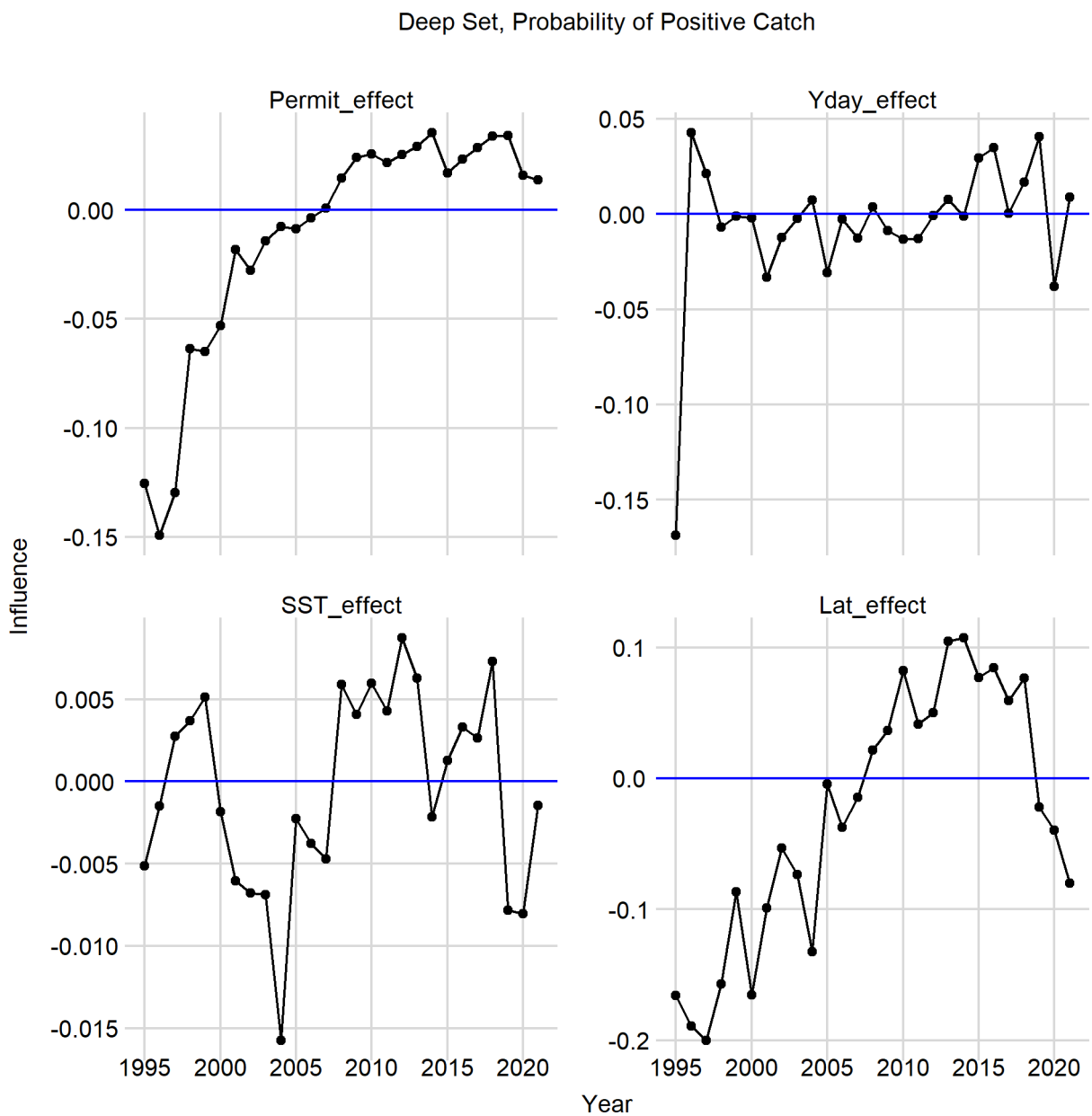


Figure 31. Deep-set 1995–2021 presence/absence influence over time of each GAMM covariate.

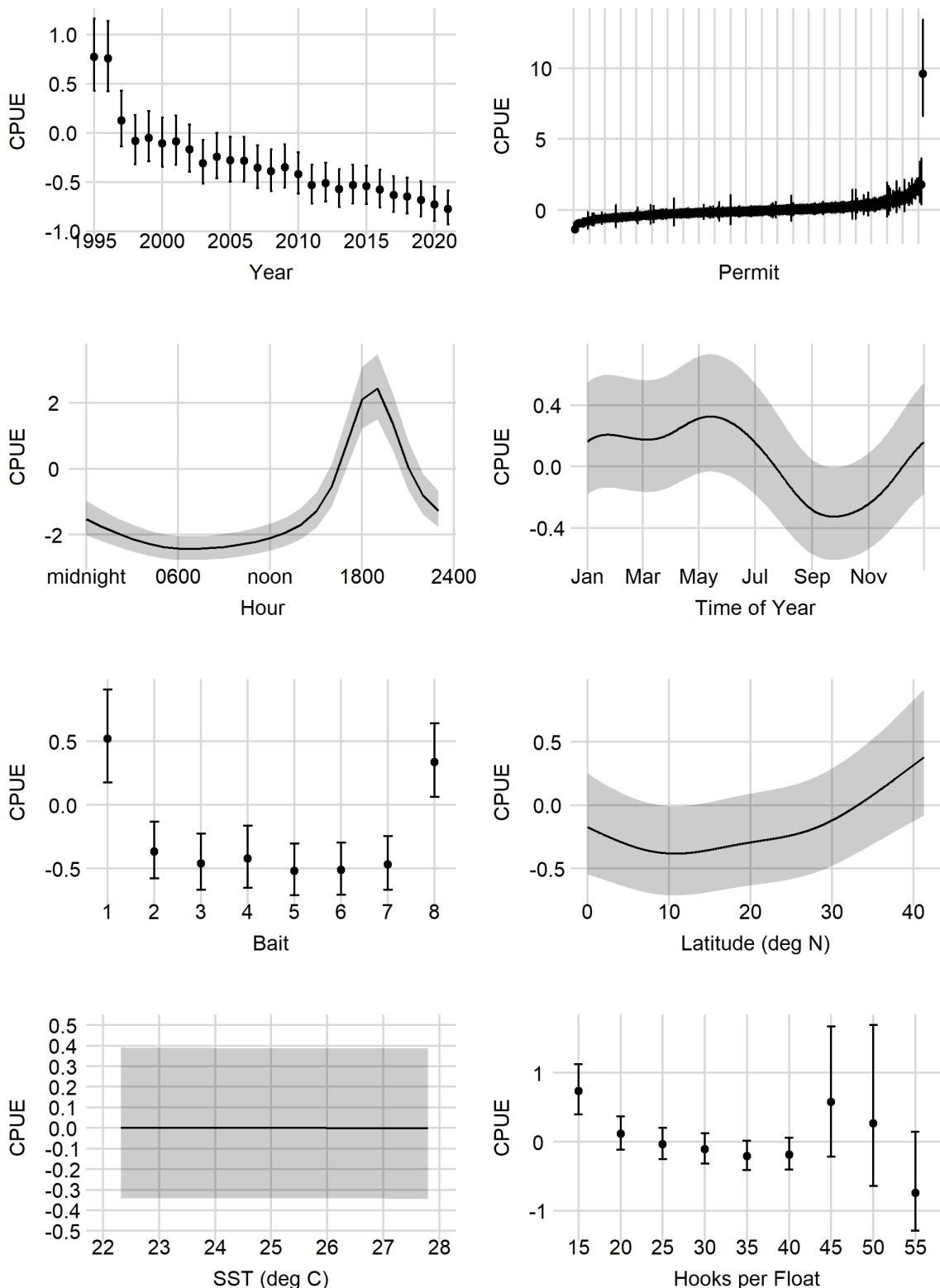


Figure 32. Deep-set 1995–2021 positive process marginal effects of each GAMM covariate. Error bars and shaded areas represent 95% confidence intervals. Bait type categories are (1) mackerel, (2) various mixed species (including various combinations of squid, mackerel, saba, sanma, sardine, akule, opelu, and herring), (3) all other species or unknown baits, (4) saba, (5) sanma, (6) sanma/sardine mix, (7) sardine, and (8) squid. Hooks per float (HPF) are given as the lower edge of each bin. A total of 30 deep-sets over the time-series where HPF = 14 were included in the first bin.

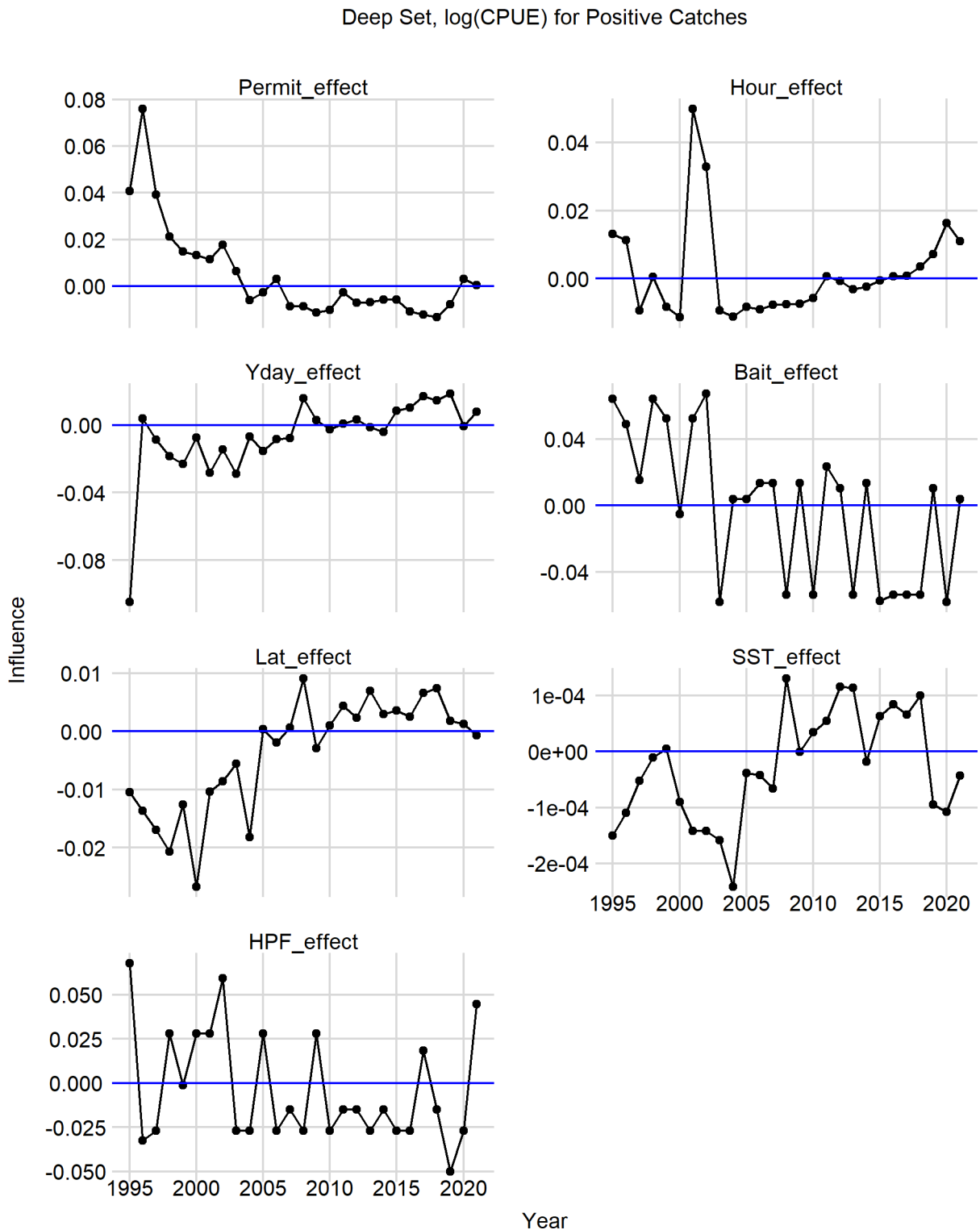


Figure 33. Deep-set 1995–2021 positive process influence over time of each GAMM covariate.

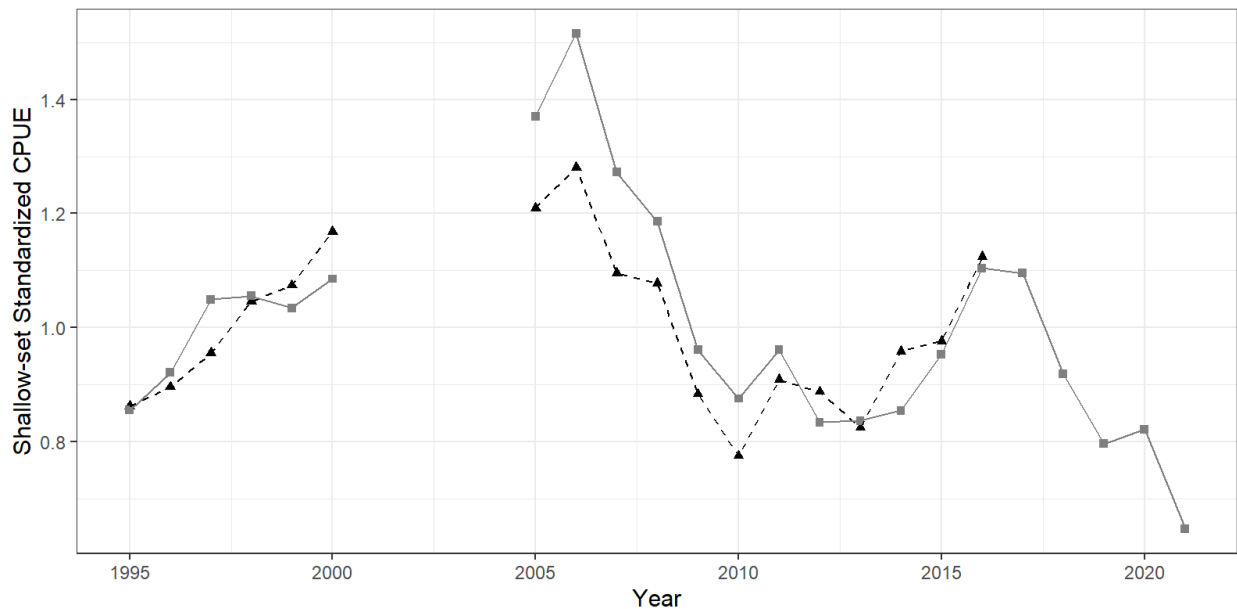


Figure 34. Comparison of standardized CPUE from the Hawai'i longline shallow-set sector from 2018 (black dashed line) and this analysis (grey solid line). CPUEs have been centered to the mean for comparison.

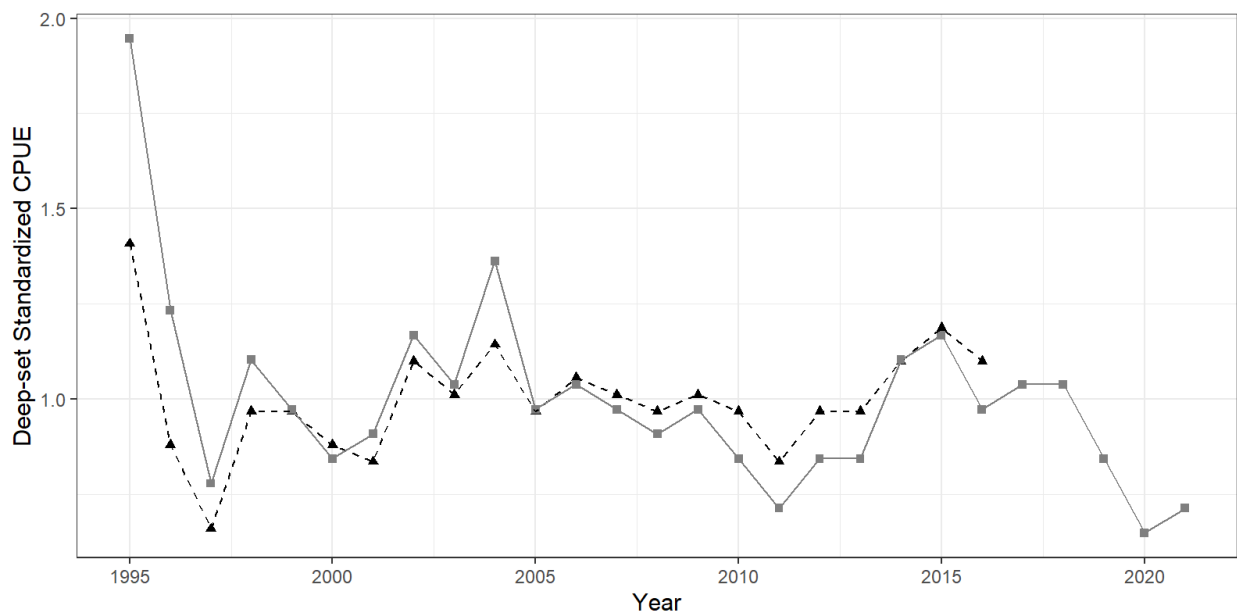


Figure 35. Comparison of standardized CPUE from the Hawai'i longline deep-set sector from 2018 (black dashed line) and this analysis (grey solid line). CPUEs have been centered to the mean for comparison.